

**PHYSICAL VAPOR DEPOSITION METHODS
FOR FABRICATING DIELECTRIC GRATINGS**

by

Morgan Edward McElhiney

A thesis submitted to the Faculty of the University of Delaware in partial fulfillment of the requirements for the degree of Master of Science in Electrical and Computer Engineering

Fall 2017

© 2017 Morgan McElhiney
All Rights Reserved

**PHYSICAL VAPOR DEPOSITION METHODS
FOR FABRICATING DIELECTRIC GRATINGS**

by

Morgan Edward McElhiney

Approved: _____
Dennis W. Prather, Ph.D.
Professor in charge of thesis on behalf of the Advisory Committee

Approved: _____
Kenneth E. Barner, Ph.D.
Chair of the Department of Electrical and Computer Engineering

Approved: _____
Babatunde A. Ogunnaike, Ph.D.
Dean of the College of Engineering

Approved: _____
Ann L. Ardis, Ph.D.
Senior Vice Provost for Graduate and Professional Education

ACKNOWLEDGMENTS

I would like to thank the numerous colleagues, friends, and family who have helped and supported me in my education, research, and career. I would like to thank Dr. Dennis Prather who has given me more support and guidance than I could have hoped for through the years as an advisor, teacher, leader, and most importantly as a mentor. I would also like to thank Dr. Mark Mirotznik for direct guidance on my work in furthering my electromagnetics research and education. I would like to thank Dr. Mathew Zablocki for years of training and guidance in the field of optics and fabrication as well as Dr. Ahmed Sharkawy and Dr. Timothy Creazzo at Lumilant Inc. for offering me invaluable experience to further bolster the scope of my knowledge as an intern.

I would also like to thank Victoria Carey for working alongside me and helping me with simulation efforts as well as fabrication for the whole extent of this project. Finally, I would like to thank Christopher Cullen, Jonathan Jerothe, Janusz Murakowski, and the entirety of Dr. Prather's research group for their help, and most importantly, my family and friends for their life long support and guidance.

TABLE OF CONTENTS

LIST OF FIGURES	vi
ABSTRACT	ix

Chapter

1	INTRODUCTION TO PHYSICAL VAPOR DEPOSITION	1
1.1	Vacuum and Plasma Sciences	2
1.1.1	Mean Free Path	2
1.1.2	Gas Flow	4
1.1.3	Vacuum Pumps and Pressure Measurement.....	4
1.1.4	Ionic Plasmas	6
1.2	UV Photolithography.....	6
1.2.1	Spin Coating	7
1.2.2	Photomasks and Mask Design	8
1.2.3	Contact Mask Alignment.....	9
1.2.4	Development and Pattern Transfer	10
1.3	Evaporation.....	11
1.3.1	Evaporation Physics	12
1.3.2	Resistive Thermal Evaporation	13
1.3.3	Electron Beam Evaporation.....	14
1.3.4	System Geometry	15
1.4	Sputtering	15
1.4.1	Sputtering Physics	16
1.4.2	Step coverage.....	17
2	ÅNGSTROM ENGINEERING™ DEPOSITION SYSTEMS	18
2.1	Åmod Electron-Beam Evaporation System.....	18
2.1.1	Safety and System Checks.....	19
2.1.2	Basic System Operation	24
2.1.3	Ångstrom Engineering System and Software.....	29
2.1.4	Inficon Deposition Software.....	39

2.2	Åmod Sputtering System.....	50
2.2.1	Safety and System Checks.....	51
2.2.2	Basic System Operation	53
2.2.3	Ångstrom Engineering System and Software.....	55
2.2.4	Inficon Deposition Software.....	63
3	PVD APPLICATIONS.....	65
3.1	Longwave Material Deposition	65
3.1.1	Germanium and Zinc Selenide	65
3.1.2	Longwave Material Deposition	67
3.1.3	Grating Fabrication.....	71
	REFERENCES	74

LIST OF FIGURES

Figure 1.1: Complimentary alignment marks drawn using AutoCAD™	9
Figure 1.2: Illustration of a liftoff process	11
Figure 1.3: Kurt J. Lesker Alumina coated dimple boat.....	13
Figure 1.4: Electron Beam evaporation system. Z.Y. Nuru et. al.....	14
Figure 2.1: Ångstrom Åmod e-beam Evaporator at University of Delaware.	19
Figure 2.2: High voltage warning on front of Åmod e-beam evaporator.	19
Figure 2.3: Windows in e-beam source cover for grounding.	20
Figure 2.4: Haskris chiller with normal temperature and no alarms.....	21
Figure 2.5: Illustration of the chiller outlet pressure gauge.	22
Figure 2.6: Helium Pressure gauge on He Compressor.	23
Figure 2.7: Roughing pump with appropriate oil level.....	23
Figure 2.8: Front panel of the Inficon Crucible Indexer.....	24
Figure 2.9: Front panel of the e-beam control unit.	25
Figure 2.10: Indicator panel for the e-beam Sweep Controller	25
Figure 2.11: Front panel of the Telemark Power Supply.....	26
Figure 2.12: Front panels of the right rack-mount units.	27
Figure 2.13: Flow switch on e-beam chilled water line.....	28
Figure 2.14: Illustration of the pneumatic and vent pressure regulators.	28
Figure 2.15: Flow diagram on the Ångstrom Engineering Software home page.	29
Figure 2.16: Diagram of the Temperature and Pressure Setpoints Menu.....	30
Figure 2.17: Diagram of the System Interlocks menu.	31
Figure 2.18: Drawing of the Source Detail and Shutter control menu.	32

Figure 2.19: Diagram of the Chamber Vent pop-up menu.	33
Figure 2.20: Unlatched chamber (left) before and (right) after reaching atmosphere.	34
Figure 2.21: Illustration of e-beam chamber with crucibles and thermal sources.	35
Figure 2.22: Illustration of the sample holder mounted and unmounted on table.	36
Figure 2.23: Side view of sample plate mount with springs and spacer screw.	37
Figure 2.24: Drawing of system state during rough vacuum pumping.	38
Figure 2.25: Capture of the Inficon Software Home Page.	39
Figure 2.26: Capture of the General Film Selection in Film Menu.	40
Figure 2.27: Capture of the Film Label Editor.	41
Figure 2.28: Capture of the Deposit Film Menu.	41
Figure 2.29: Screen Shot of the Deposit Condition Menu.	42
Figure 2.30: Capture of the Source/Sensor Menu.	43
Figure 2.31: Screen capture of the Errors Menu.	45
Figure 2.32: Screen shot of Process Menu with Layer Tab Selected.	46
Figure 2.33: Screen capture of the Rate Ramps Tab.	47
Figure 2.34: Screen capture of the Change Process Prompt.	48
Figure 2.35: Screen capture of the Sensor Life Readings.	49
Figure 2.36: Illustration of the Åmod Sputtering System.	50
Figure 2.37: Illustration of the Thermoflex 5000 chiller on Sputter chiller loop.	51
Figure 2.38: Pictures of (left) Oxygen and Argon Tanks and (right) Nitrogen Tank.	52
Figure 2.39: Illustration of the Substrate heater controller.	53
Figure 2.40: Front panel of the DC Sputtering Source.	53
Figure 2.41: Front panel of the RF Matching unit.	54

Figure 2.42: Front panel of the RF Sputtering Source.....	54
Figure 2.43: Front panel of the VAT Adaptive Pressure Controller.....	55
Figure 2.44: Drawing of the Sputter System Home Page.....	56
Figure 2.45: Screen capture of the Gas Recipe Setup Menu.	57
Figure 2.46: Screen capture of the Gas Properties Setup Menu.	57
Figure 2.47: Drawing of the Sputter System Source Detail and Shutter Control Menu.....	58
Figure 2.48: Image of the Sputtering Targets and Crystal Sensors.	59
Figure 2.49: Illustration of the Secondary Target Collar.	60
Figure 2.50: Demonstration of Target Removal.....	60
Figure 2.51: Demonstration of Checking Collar Gap with Spacer.	61
Figure 2.52: Illustrations of (left) Sample Plate and (right) Quartz Lamp Heaters.	62
Figure 2.53: Screen capture of the Sputterer Layer Tab.....	63
Figure 3.1: Plot of the Refractive Index of Ge.....	66
Figure 3.2: Plot of the Refractive Index of ZnSe.....	67
Figure 3.3: Illustration of the Covap II Thermal Evaporator.....	68
Figure 3.4: SEM of Warped ZnSe Cantilevers from Film Stress Gradients.....	71
Figure 3.5: SEM of a 1D Germanium Grating.	73
Figure 3.6: SEM of a 2D Germanium Grating.	73

ABSTRACT

There are many tools necessary in the construction of structures utilizing nanofabrication processes. Some of these tools are subtractive, such as etching which removes material from the device. Others are additive such as electroplating, chemical vapor deposition, and physical vapor deposition. This thesis will thoroughly explore two common physical deposition methods, Evaporation and Sputtering. These methods are used in our labs to deposit metals, semiconductors, and insulators. These processes are highly system dependent and require in depth process development and system understanding. To fully explain the physical vapor deposition techniques used for construction of many devices, the physical and mechanical processes will be discussed as well as the standard operating procedures required for operating the three physical deposition systems in the Electrical and Computer Engineering clean room located in DuPont Hall at the University of Delaware. These systems were used to deposit clean, uniform, and precise films of optical dielectric material to form candidate nano-scale profiles, which for the purpose of illustration consist of gratings in this thesis.

Chapter 1

INTRODUCTION TO PHYSICAL VAPOR DEPOSITION

One of the earliest needs in micro-circuit fabrication was to reliably deposit chip-scale wires to form circuits. These wires, comprised of various metals, are used to carry current from off-chip to various components and to interconnect various components to form usable circuit networks. To form such reliable thin films of metals and later dielectric materials, two major methods of physical vapor deposition (PVD) are used: evaporation and sputtering. PVD processes use thermal and mechanical methods to coat samples, as opposed to Chemical Vapor Deposition (CVD) processes, which rely on a chemical reaction to grow a film of material. The advantage of using a PVD process rather than a CVD process is that PVD processes mostly do not require high substrate temperatures to facilitate a reaction and therefore introduce fewer film stress gradients due to differing coefficients of thermal expansion (CTE). A drawback to PVD processes is the risk of substrate crystalline structure damage due to the high velocity molecules hitting the substrate [1].

PVD processes, especially evaporation, have specific chamber pressure and source temperature requirements; therefore, it is important to maintain reliable environmental conditions during the deposition processes. It is also commonly desired to pattern the deposited films. To achieve patterns in nano- and micro-structures various forms of lithography are used. This chapter is designed to give a textbook understanding of basic micromachining processes used in realization of patterns

utilizing PVD films. It will cover basic vacuum and plasma sciences, ultra violet (UV) photolithography, evaporation, and sputtering.

1.1 Vacuum and Plasma Sciences

Although some processes used in the fabrication of micro-structures are performed in a normal atmospheric laboratory environment, many are performed at extremely low pressures. A vacuum environment facilitates not only clean, dry, inert, and reliable experimental conditions, but also allows for molecules to travel uninhibited through space. Low pressure gasses can be manipulated through electric fields to ionize into plasmas and be accelerated toward samples or material sources to sputter away the material for etching or PVD processes.

1.1.1 Mean Free Path

To better understand how gas molecules propagate through free space, statistical models are used to estimate how a molecule travels. Assuming gas molecules are hard spheres, the probability distribution of velocities is given by the Maxwell speed distribution:

$$P(v) = 4\pi \left[\frac{m}{2\pi kT} \right]^{\frac{3}{2}} v^2 e^{-mv^2/2kT}, \quad (1.1)$$

where m is the molecule mass, v is the magnitude of velocity, k is Boltzmann's constant and T is the temperature in Kelvin. The average magnitude of velocity is given by

$$|v| \equiv \bar{c} = \int_0^{\infty} v P(v) dv = \sqrt{\frac{8kT}{\pi m}} \quad (1.2)$$

The average component of the velocity in any direction is given by the equipartition theorem:

$$\overline{v_x} = \overline{v_y} = \overline{v_z} = \sqrt{\frac{2kT}{\pi m}}, \quad (1.3)$$

and the root mean square velocity is given by

$$v_{rms} = \sqrt{\frac{3kT}{m}} \quad (1.4)$$

The nature of gasses due to thermal velocity is random in direction if no external forces are applied. At equilibrium, the average velocity is zero. If a pressure gradient is applied, the random movement of the molecules will drift or diffuse toward the lower pressure area.

In vacuum systems, it is important to understand the probability that one molecule will hit another molecule. Using the statistical model for the velocity of a molecule we can estimate the probability of a collision over distance L as:

$$P \approx L\pi d^2 n, \quad (1.5)$$

Where n is the number of present atoms with diameter d . Assuming a probability of one we can derive an average distance between collisions, or the mean free path as:

$$\lambda \approx \frac{1}{\sqrt{2}\pi d^2 n} \quad (1.6)$$

Substituting for n , using the ideal gas law we can better understand the mean free path as a function of pressure and temperature:

$$\lambda = \frac{kT}{\sqrt{2}\pi d^2 P} \quad (1.7)$$

These equations only apply when $\lambda \ll L$, also called the viscous flow regime. L is defined as the characteristic length of the chamber [2].

1.1.2 Gas Flow

Although the inherent nature of gasses is to move randomly, collisions cause the gasses to flow. Gasses are more compressible than liquids, so a throughput model is used. Gas throughput Q , is measured in terms of volume that it would occupy at 1 atm of pressure at 0° C. As gas flows from a chamber of high pressure to a chamber of lower pressure through a tube of finite diameter, the conductance of the tube must be considered,

$$C = \frac{Q}{P_1 - P_2} \quad (1.8)$$

Tube conductance adds similarly to electrical conductance given by:

$$\frac{1}{C_{series}} = \frac{1}{C_1} + \frac{1}{C_2} + \frac{1}{C_3} + \dots \quad (1.9)$$

Therefore, increasing the diameter of the tube or increasing the number of tubes will increase the gas flow and subsequently pump down speed [3].

1.1.3 Vacuum Pumps and Pressure Measurement

A vacuum is defined as a space absolutely devoid of matter. Since outer space isn't even completely devoid of matter, vacuum environments are defined by how well they represent a vacuum. Vacuum regions are approximated by the technology used to create such an environment [1]. A rough vacuum is approximated as from 760 torr - 0.1 torr, medium vacuum from 10^{-1} torr - 10^{-4} torr, high vacuum as 10^{-4} torr - 10^{-8} torr, and ultrahigh vacuum as less than 10^{-8} torr. Different vacuum pumps are used to achieve these various ranges.

Rough vacuum pumps are used to achieve rough and medium vacuums. They are mechanical pumps, which utilize pistons, vanes, plungers, or diaphragms to positively displace gasses. Rough pumps have three steps of operation. They capture a

gas at the inlet, compress the gas, and then release the gas from a separate outlet. Although these pumps cannot achieve high vacuum levels, they are ideal for use starting at atmospheric pressure. This makes them useful in applications where the pump might be exposed to atmosphere such as securing substrates on a vacuum chuck or preparing a chamber to be pumped down further by a more complex pump.

Turbomolecular pumps (TMPs) are pumps that contain multiple stages of spinning fan blades, which spin at high speeds. Between each rotating blade set is a stationary set of blades, which introduce a modest compression ratio. A single stage TMP would not be an impressive vacuum pump, but the combination of many stages gives massive compression ratios allowing for some TMPs to achieve ultrahigh vacuum. TMPs are not typically designed to operate at atmospheric pressure and typically work in conjunction with a roughing pump, which is attached to the exhaust of the TMP. When operated properly TMPs are very clean [1].

Gas entrainment pumps are even cleaner than TMPs. The most commonly used gas entrainment pump in microelectronics processing is the cryopump. Cryopumps operate by cooling the pump head to temperatures below 20 K. This traps gasses other than He by freezing them, thus removing them from the air. Cryopumps are consequently cooled by a He compressor by pumping high pressure He into the inlet and returning low pressure He to the compressor to be cooled and recompressed. Cryopumps build up frozen gasses on the head and need to be regenerated by isolating the pump and heating it to room temperature thereby releasing any trapped gasses [4].

Pressure, within a vacuum system is measured by various gauges. Common gauges include capacitance manometers and ionization gauges. Capacitance manometers, or diaphragm gauges, consist of a mechanical type of gauge that detects

the movement of a thin film, or diaphragm, due to the difference of pressure between the chamber and a reference volume. They are typically used in rough vacuum environments. Ion gauges are used for measuring high and ultrahigh vacuum. They operate by emitting an electron beam to ionize the gas and an electric field to collect the charges. The subsequent current is directly related to the pressure in the chamber [1].

1.1.4 Ionic Plasmas

A plasma is defined as a partially ionized gas. It is a special state of matter, which emits light known as a glow discharge. Plasmas are used to either disassociate molecules or to create and accelerate ions. A simple plasma system is defined by a parallel plate capacitor in a chamber with an inlet gas and a pressure maintaining pump. The voltage on the capacitor is increased until the electric field across the gas exceeds its breakdown voltage causing a current to arise between the plates. This causes electrons to accelerate toward the anode defining a current, and ions to be accelerated toward the cathode.

When electrons collide inelastically with a neutral molecule, the electrons can be excited to a higher energy state. This state is short lived. As the electron falls back to its ground state the energy is released in the form of a photon, thereby emitting light [5]. DC voltages can only be applied if both charged surfaces are metals. If either of the surfaces is coated or blocked by an insulator, RF fields must be applied.

1.2 UV Photolithography

Thin film deposition is useful when it is possible to realize patterns in those films. Patterns in nanofabrication are developed in several ways. Most methods

involve photo-sensitive polymers known as photoresist. When light is projected through a mask pattern onto the photoresist to develop a pattern, it is known as photolithography. Types of photolithography include gap photolithography, contact photolithography, projection photolithography, and immersion photolithography. Photolithography is limited by half the wavelength of the projected light by diffraction. Typical UV photolithography can potentially resolve features down to ~130 nm, but this can be reduced further by immersing the system in a high index material to spatially reduce the wavelength of the incident light.

Other ways of exposing photoresist include e-beam lithography, x-ray lithography, and laser lithography some of which can resolve features down to 10 nm. This section will primarily focus on contact UV photolithography processes including polymer spin casting, mask design and application, UV exposure, development, and pattern transfer.

1.2.1 Spin Coating

A third method of depositing thin films, other than CVD and PVD processes, is spin coating. This process is performed with polymers suspended in solvents, especially photoresists. Cleanliness is crucial in producing uniform reliable films; therefore, wafers and samples are thoroughly cleaned in solvents, acids, and/or oxygen plasmas to remove any debris or organic material from the surface. Solvent cleans can be performed as a part of the spinning process.

Spin coating works by rapidly spinning a sample covered in an excess amount of photoresist suspended in a specific amount of solvent. As the sample spins, the centripetal force drives the solution away from the center point; a thin film is left behind. The thickness of the resulting film is dependent on the solvent concentration

in the photoresist. Viscous solutions result in thicker films. Spin speed also contributes to the film thickness, as speeds increase, the centripetal force on the polymer also increases creating thinner films.

Futurrex™ NR9 is a commonly used negative photoresist. The following process is one way to form a clean and reliable NR9 film on a silicon substrate. A silicon sample is mounted and centered on a well-balanced vacuum chuck attached to a spin coater's spindle. The spindle then accelerates to 3,000 rpm. While the sample is spinning, acetone, methanol, and isopropanol are sprayed for approximately 7s each from wash bottles in the order listed to thoroughly clean the sample. It is important to not allow the sample to dry between solvents, as acetone and methanol leave behind residue if not washed away by isopropanol. The spindle then accelerates to 4,000 rpm, for 20s, to dry the sample. After the sample is dry, the spindle stops to allow for the NR9 to be pipetted onto the sample. For this example, and all subsequent examples, NR9-1500PY will be used. The spindle is once more accelerated to a speed of 3,000 rpm at a rate of 1,000 rpm/s for 45s. This is the spin casting step and the speed, rate, time, and resist type define the resulting film. NR9 1500, when spun at 3,000 rpm, will result in a film of approximately 1.5 μm . The sample is removed, then soft baked on a hot plate at 150° C for 60s to remove any remaining solvent. The photoresist still needs to be patterned.

1.2.2 Photomasks and Mask Design

To define features in photoresist, a physical device called a photomask is utilized. Masks are typically made from soda lime glass or quartz. Quartz is used when deep UV (DUV) light is required to resolve smaller features. Soda lime glass is cheaper but does not transmit DUV light well. One side of the mask is coated in a

thick chromium film. This film is patterned by laser lithography, e-beam lithography, or other methods, and then etched. The resultant Cr features are used to block light in some areas, whereas the gaps transmit light.

When designing a mask, it is important to understand that the pattern on the mask will not be identical to the mask, due to diffraction, especially for small features $\lambda \approx D$. Multiple patterns for the same device can be patterned on the same mask. These patterns can be overlaid to form complex structures from multiple films or etches. Aligning these structures is important. Incorporating complimentary alignment marks on a sample allow for precise layer alignment. An example of complimentary alignment marks for multiple layers is shown in Fig. 1.1.

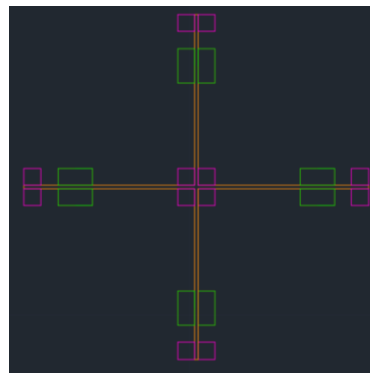


Figure 1.1: Complimentary alignment marks drawn using AutoCAD™

1.2.3 Contact Mask Alignment

Now that the sample is coated in photoresist and a pattern is prepared on a photomask, the pattern needs to be transferred to the photoresist. To achieve this, UV light is projected through the photomask onto the photoresist. With positive photoresist, the polymer chains are naturally crosslinked and exposure to UV light will

delink the chains. Negative photoresists, such as NR9, are the opposite and naturally not crosslinked, but will be crosslinked when exposed to UV light and subsequently baked. Exposure dose is dependent on resist thickness, critical feature size, and resist type.

Contact mask aligners are simple. They consist of a light source with mirrors and optics to project collimated light of specific wavelengths uniformly across a photomask. The photomask is pressed onto the photoresist layer of the sample and the entire assembly is put under a rough vacuum to decrease the space between the mask and the resist. Though the gap is small, it is not negligible. Smaller gap sizes are preferred because the light will diffract off the photomask at an angle reducing your pattern transfer precision. Gap size is dependent on photoresist uniformity, sample cleanliness, and careful leveling and suction. The probability of good contact can be increased by removing the polymer edge bead from the sample and blowing the surface of the sample with compressed nitrogen.

1.2.4 Development and Pattern Transfer

Once the photoresist has been exposed, the film needs to be developed to wash away the undesired sections. Crosslinked sections are more resistant to developer solutions and wash away significantly slower than nonlinked sections. The solution realizes the features by using this ratio to its advantage. Linked sections are mostly untouched where unlinked sections are rapidly dissolved leaving the desired image. These patterns are then easily used to serve as a barrier for wet etching, dry etching, diffusions, and as sacrificial layers during physical vapor deposition (PVD) processes.

One specific process that is achieved using NR9-1500PY is called liftoff. The nature of this resist is to create sidewalls that are slightly undercut. The undercut

makes the base of the photoresist layer narrower than the top layer. This discontinuity allows for materials to be deposited between, and on top, of the photoresist sections. If the resist layer is considerably thicker than the deposited layer, the material on top of the resist will not connect to the resist on the sample. This allows for the photoresist to be washed away by solvents lifting off the material in resist coated areas, see Fig. 1.2.



Figure 1.2: Illustration of a liftoff process

1.3 Evaporation

The earliest form of PVD was evaporation. Evaporation is a simple process that relies on heating a material until it reaches a vapor point. Since evaporation processes are performed under high vacuum conditions, the vapor pressure will cause the material to travel across the chamber and coat the opposing surface. The material being consumed for deposition is known as the charge. The charge is heated in many ways. The two ways of heating a charge presented here, are simple resistive heating and electron beam heating. This section will cover the physics behind evaporation, thermal evaporation, electron beam evaporation, and system geometry.

1.3.1 Evaporation Physics

When considering a material for evaporation, the phase diagram of the material is crucial for determining the conditions necessary for deposit. A phase diagram maps the stability of a material at various temperatures and pressure. This stability determines the state of the material. As temperature increases materials transition through solid, liquid, and gas state changes. In evaporation, we are concerned with the state change from liquid to gas. With some materials, such as chromium, the vapor point is below the melting point. This causes the material to skip the liquid phase in a process called sublimation. The rate of deposition is highly dependent on vapor pressure. Vapor pressure, P_e , is given by:

$$P_e = 3 \times 10^{12} \sigma^{3/2} T^{-1/2} e^{-\Delta H_v / NkT} \quad (1.10)$$

Where σ is the surface tension, N is Avogadro's number, and ΔH_v is the enthalpy of evaporation. To achieve legitimate deposition rate, vapor pressures of at least 10 mtorr must be achieved. The flux rate to determine the number of gas molecules crossing a plane:

$$J_n = \sqrt{\frac{P^2}{2\pi kTm}}, \quad (1.11)$$

where P is the pressure in the chamber and m is the atomic mass, is multiplied by the mass of the molecule to produce the Langmuir evaporation rate:

$$R_{ME} = \sqrt{\frac{m}{2\pi kT}} P_e \quad (1.12)$$

Assuming the entirety of the charge is molten and at constant temperature, and the opening of the crucible has finite area, A , the evaporation rate can be defined as:

$$R_{ME} = \sqrt{\frac{m}{2\pi kT}} P_e A, \quad (1.13)$$

which is the total amount of material leaving the crucible [6].

1.3.2 Resistive Thermal Evaporation

Thermal evaporation is the simplest form of heating a charge. A metal rod or boat, typically made of tungsten, molybdenum, or tantalum, is clamped to a voltage source and a ground. The voltage source induces a current through the resistive metal based on Ohm's law and heats a rod or boat. Rods, typically coated in Chromium, heat and sublime the material from the surface. A molten charge would not work for this configuration because the material would drip. To contain a molten material, a resistive boat is used. To reduce contamination and boat destruction from CTE mismatches, boats are often coated in Alumina films. Alumina has a high melting point and coefficient of thermal conductivity.



Figure 1.3: Kurt J. Lesker Alumina coated dimple boat

1.3.3 Electron Beam Evaporation

Although simple and economical, thermal evaporation has drawbacks. It is often unreliable and leads to charge contamination. Boats and rods also have a short lifespan, typically on the order of ten depositions. To achieve cleaner more reliable depositions crucibles heated by electron beams are deployed. In this case, a hot wire filament serves as an electron source, and the electrons are accelerated and then focused by controllable electromagnets. These magnets direct the electron beam towards the charge located in a crucible to create a uniform melt. The beam is raster scanned across the crucible surface to heat a larger surface area [1].

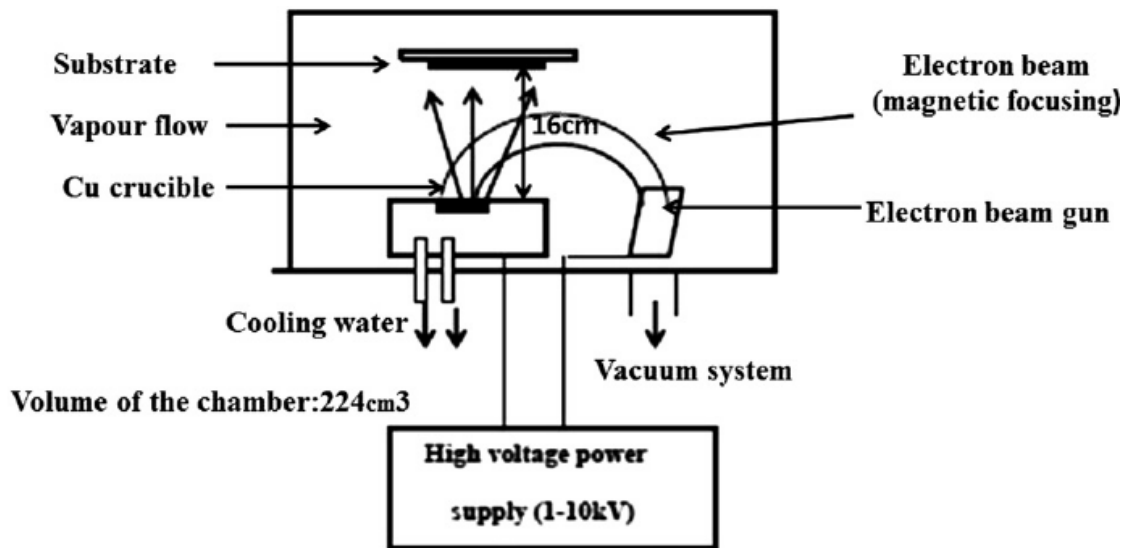


Figure 1.4: Electron Beam evaporation system. Z.Y. Nuru et. al.

A major advantage of e-beam evaporation is material isolation. Even though the goal of evaporation is to heat the charge, e-beam crucibles are cooled. This allows for a melt to exist near the location of the electron beam, but the rest of the material

can remain solid. This boundary is desired to contain the material without contaminants leaching from the crucible.

1.3.4 System Geometry

After exploring the methods of heating and physics behind evaporation, it is important to note that not all the material leaving the crucible will coat the intended target. Assuming an arbitrary geometry, the radiation of material can be assumed to be spherically divergent:

$$\cos \theta = \cos \varphi = \frac{R}{2r}, \quad (1.14)$$

where R is the distance from the crucible and r is the distance from the center of the arbitrary sphere. Using this assumption, the arrival rate per unit area divided by the mass density of the film, ρ , can be updated as:

$$R_d = \sqrt{\frac{M}{2\pi k \rho^2 T}} \frac{P_e A}{4\pi r^2} \quad (1.15)$$

It is possible to calculate a potential deposition rate theoretically, but typical rates and processes are developed empirically. If large angles away from the normal of the crucible are not required and samples are placed in generally the same location for each run, crystal rate monitors can be tooled and calibrated by physically measuring a test film's thickness using optical or atomic force methods.

1.4 Sputtering

Evaporation is a useful method for depositing reliable thin films for microscale fabrication, but it is often slow, high temperature, and has poor step coverage. Sputtering was developed as a thin film deposition method in the 1920s. Sputtering

utilizes plasmas to deposit material. This section will describe the physics of sputtering as well as step coverage and film conformity differences between evaporation and sputtering.

1.4.1 Sputtering Physics

Sputtering relies on plasmas to accelerate ions toward a target material. The high energy of these accelerated molecules bombards the surface. At low energy, ions will bounce off the surface or be absorbed as heat. At extremely high energies the ions will burry themselves, or implant deep into the material. High energy implantation is used for precise semiconductor doping processes. At median energies, a combination of these two mechanisms will be present. This causes surface molecules to be ejected from the target.

When developing a sputtering process, the number of atoms ejected from the target, which leads to deposition rate, is known as sputtering yield. The current of atoms ejected is related to the ion flux approximated by the Langmuir-Child relationship:

$$J_{ion} \propto \sqrt{\frac{1}{m_{ion}}} \frac{V^{3/2}}{d^2}, \quad (1.16)$$

where, V is the voltage difference, d is the dark space thickness, and m_{ion} is the mass of the ion. Many material sputtering rates are angularly dependent based on crystal structure. The angularly dependent sputter yield is approximated as:

$$S \propto \frac{M_{gas}}{M_{target}} \frac{\ln E}{E} \frac{1}{\cos \theta} \quad (1.17)$$

Thus, the deposition rate can be calculated by [8]:

$$R_d = \frac{J_{ion} * S * E_T}{\rho / m}, \quad (1.18)$$

where E_T is the transport efficiency and is usually assumed to be one.

1.4.2 Step coverage

As mentioned previously while describing liftoff processes, evaporation is highly directional and capable of forming discontinuous films. This is due to the low energy apparent when the atoms reach the desired surface. Since sputtered molecules are at a higher energy state, they can move more on the surface. This enables sputtered films to conform to step height non-uniformities. Though not desirable for liftoff, it is highly desirable for electrical contacts, which need to bridge layers. Rotating the substrate increases the step coverage as well.

Chapter 2

ÅNGSTROM ENGINEERING™ DEPOSITION SYSTEMS

The focus of this chapter is to present a fundamental understanding of how PVD systems are operated; specifically, the operation of two Ångstrom Engineering PVD systems. The specific systems include the Åmod e-beam Evaporator and the Åmod Sputterer. The Covap II Thermal evaporator will be described in Chapter 3. These systems are all located in the Electrical and Computer nanofabrication facility at the University of Delaware.

2.1 Åmod Electron-Beam Evaporation System

To deposit reliable metal films for nanoelectronics devices electron-beam evaporation is crucial. To perform this task, the Åmod e-beam Evaporator (shown in Fig. 2.1) can be used.



Figure 2.1: Ångstrom Åmod e-beam Evaporator at University of Delaware.

2.1.1 Safety and System Checks

Since high voltage is required for the e-beam source, it is extremely important to ground the system utilizing the attached grounding stick immediately after opening the reaction chamber.

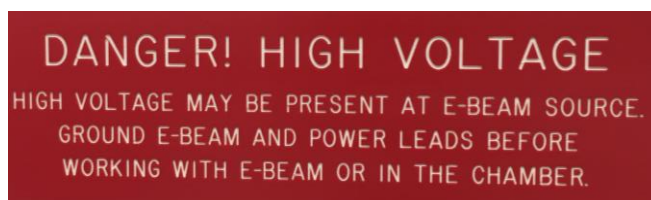


Figure 2.2: High voltage warning on front of Åmod e-beam evaporator.

The system is grounded by probing the main posts of the e-beam gun through the grounding windows on the extractor cover (circled in Fig. 2.3). It is also useful to touch the indexer plate and other sources as they might accumulate charge. Not grounding the system can result in rapid discharge of accumulated voltage leading to death or serious injury.

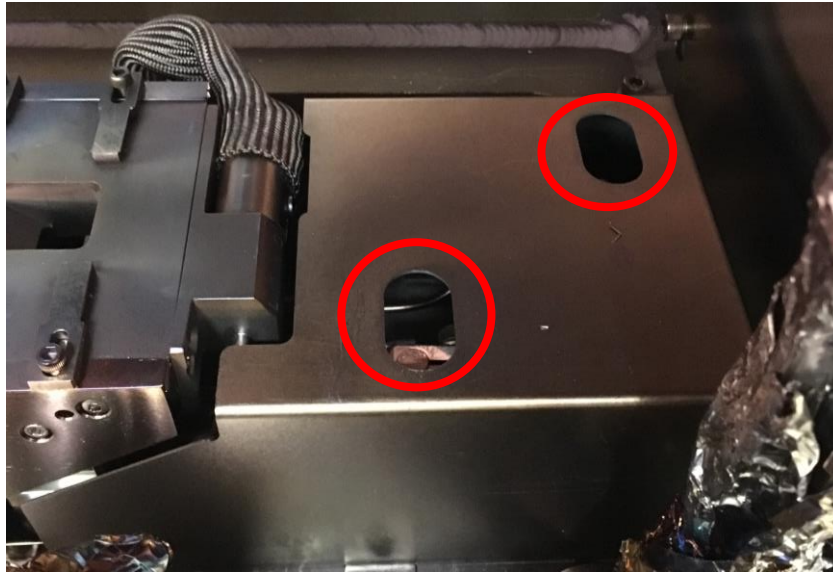


Figure 2.3: Windows in e-beam source cover for grounding.

In the back chase, there are a few auxiliary systems that need to be operating properly for the main system to function. First, is the Haskris chiller, which is the first large device, shown in Fig. 2.4.



Figure 2.4: Haskris chiller with normal temperature and no alarms.

Since this system has an automated pressure diverter, it is only important to confirm that the two temperatures, process variable (PV) and setpoint variable (SV), match and that no alarms are active. If these two values do not match, the system is not operating properly. It is also valuable to check the pressure gauge (Fig. 2.5) on the outlet line on the back of the system. This should read ~60 psi.



Figure 2.5: Illustration of the chiller outlet pressure gauge.

The next system to be checked, located between the sputterer chiller and the roughing pumps, is the He compressor. This device compresses He to remove heat from the cryopump attached to the main system. The compressor is cooled by the Haskris chiller. To confirm appropriate operation, locate the He pressure gauge, shown in Fig. 2.6, and confirm the needle is near the white line. The unit should be vibrating and the needle should be moving slightly. Finally, confirm that the oil level, on the adjacent roughing pump, is between the lines, Fig. 2.7.

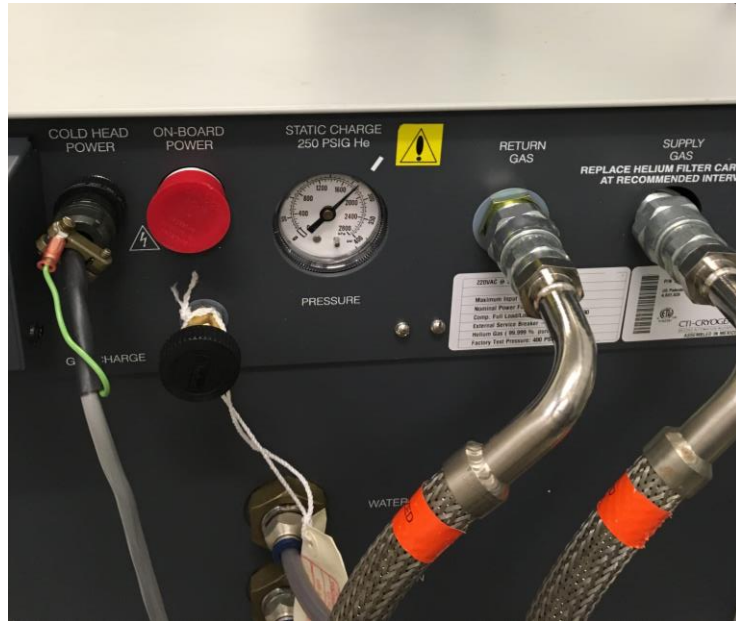


Figure 2.6: Helium Pressure gauge on He Compressor.



Figure 2.7: Roughing pump with appropriate oil level.

2.1.2 Basic System Operation

Before considering starting a deposition, it is vital to understand how all of the system components operate and how they contribute to maintain a reliable process. A large portion of these systems are housed on the front rack mount panel of the main system box, rack can be seen in Fig. 2.1. Starting at the top left rack slot is the crucible indexer Fig. 2.8.

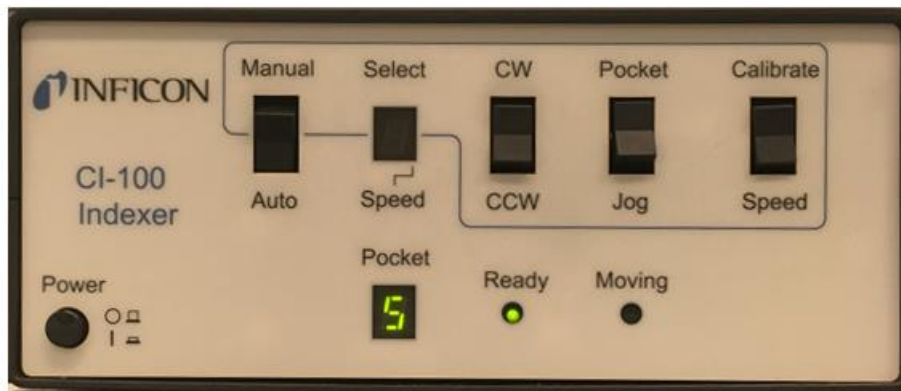


Figure 2.8: Front panel of the Inficon Crucible Indexer.

The crucible indexer controls the rotation of the six-crucible pocket wheel, located in the deposition chamber. This wheel spins to change which crucible is exposed in a particular deposition. When preparing to perform a deposition, the indexer must be on. The power button should be in the “on” position and the ready light should be illuminated. The mode switch should be in the “auto” position. The indexer should not be operated in the manual operation mode by standard users! The seven-segment display labeled “Pocket” shows the current exposed crucible. The crucible indexer can be controlled by the Ångström software while the chamber is closed. This reduces the risk of injury and damage the system.

Then next system on the rack is the e-beam control unit, Fig. 2.9.



Figure 2.9: Front panel of the e-beam control unit.

This rack unit controls the high voltage DC output of the e-beam source. The power switch must be in the “on” position, and the control select switch must be in the “remote” position for normal operation. This allows for the unit to be controlled by the Inficon software, which will be detailed in the next section. The unit displays show the source voltage and current being produced during the deposition.

The next rack unit is the e-beam sweep controller, as shown in Fig. 2.10.



Figure 2.10: Indicator panel for the e-beam Sweep Controller

This controller consists of two separate modules that plug into the main sweep controller unit. The left half is a manual controller with a joystick to control e-beam position, as well as knobs to control raster parameters. The other section is a sweep

select panel, which can have four sweeps pre-configured for selection. These sweeps can be called from the Inficon software. For normal operation, the power switch on the sweep controller must be on and the module selector switch should be set to “sweep select.” The mode switch on the sweep select panel must be on “auto.” To control the beam using the manual control unit the selector switch should be switched to “control.” Manual control should only be used when absolutely necessary. Manual sweep select should not be used.

The last unit on the left rack is the power supply, shown in Fig. 2.11.

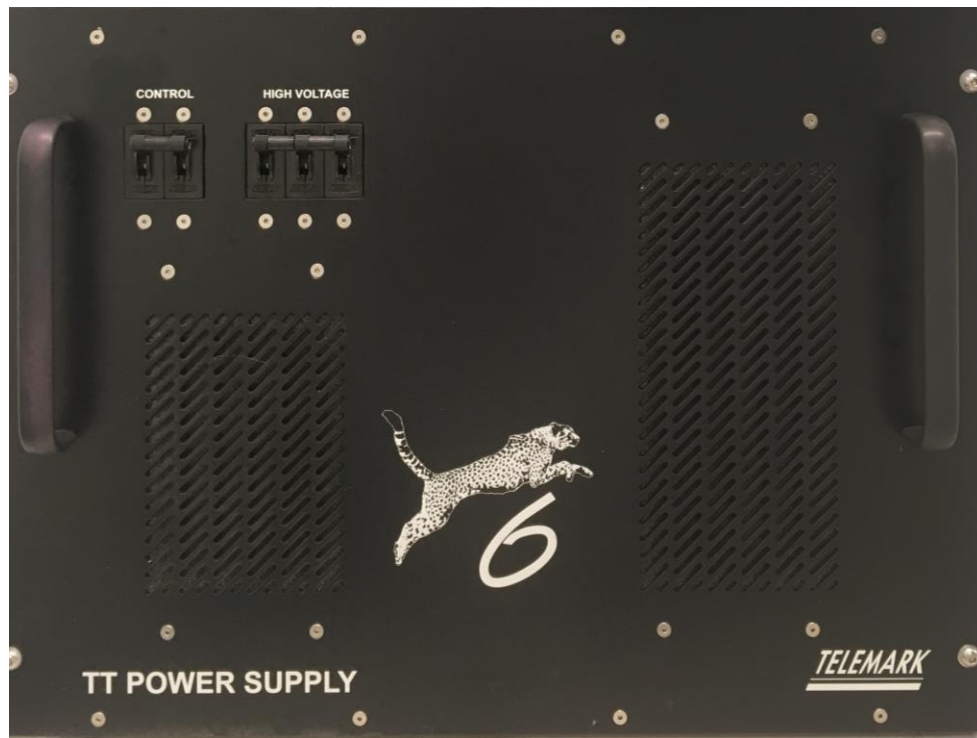


Figure 2.11: Front panel of the Telemark Power Supply.

This power source supplies the e-beam high voltage and the control units. Both sets of breakers should be in the on position.

A few more components are affixed to the right rack mount section of the system box, shown in Fig. 2.12.



Figure 2.12: Front panels of the right rack-mount units.

The red button on the top left is the emergency stop switch. This cuts power to the whole system, stopping any process. This button should only be used in a real emergency when all other processes stopping methods are not possible, as it is not a healthy way to power down the system. The next unit is the cryopump temperature controller. The display should read a value below 19 K.

The last unit in the top row is the substrate rotation controller. A dial controls the rotation speed and a switch enables or disables rotation. The controller is toggled by the start of a process.

The large black unit in the second row is the system computer and should always be left on. If the computer is off, please contact the equipment supervisor as there may be other problems with the system. Next, confirm water flow to the e-beam source by confirming the flow switch reads greater than 1.0, Fig. 2.13. The display can be seen through the handle hole on the left side of the system.

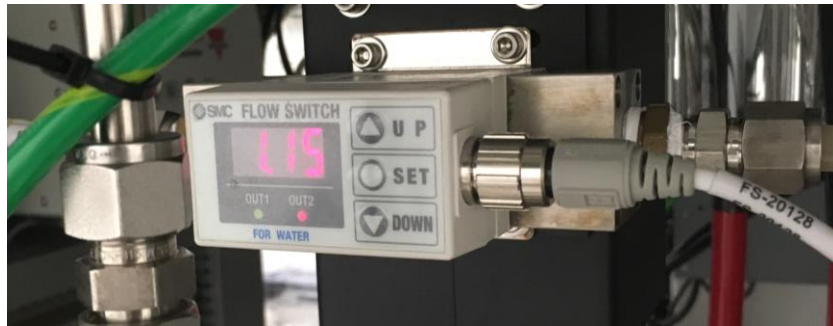


Figure 2.13: Flow switch on e-beam chilled water line.

Finally, check the pneumatic and vent line pressure regulators on the wall behind the system and confirm their pressures match the set points. The left two are for the e-beam evaporator, shown in Fig. 2.14.



Figure 2.14: Illustration of the pneumatic and vent pressure regulators.

2.1.3 Ångstrom Engineering System and Software

The system is controlled by two different software applications. The first is the system software made by Ångstrom Engineering. This application controls most of the system, including pumps, gauges, valves, shutters, substrate rotation, and the compressor. It also establishes system and safety interlocks to regulate system control to reduce damage to the system and the user. This software is access controlled, and after successfully completing training with an approved system supervisor, you will be given a username and password for the system. To login press the “LOGIN” button, then enter your specific username and password.

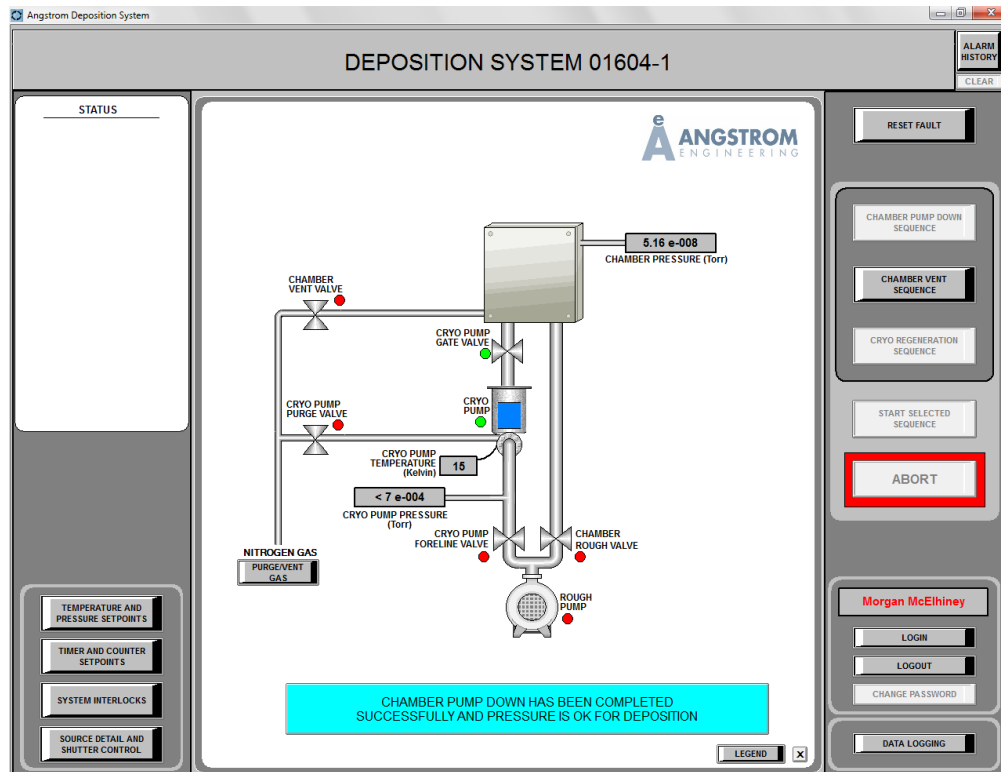


Figure 2.15: Flow diagram on the Ångstrom Engineering Software home page.

The software home page, shown in Fig. 2.15, shows the system flow diagram, which details the current system state. It shows the various pump conditions, gauge readings, and valve and interconnect positions. There are also some menus that can be accessed by clicking the buttons at the bottom left of the page. The first button, labeled “TEMPERATURE AND PRESSURE SETPOINTS,” opens a display window containing the values set for various temperature and pressure setpoints required for pump crossover, deposition, and other system processes, as shown in Fig. 2.16.

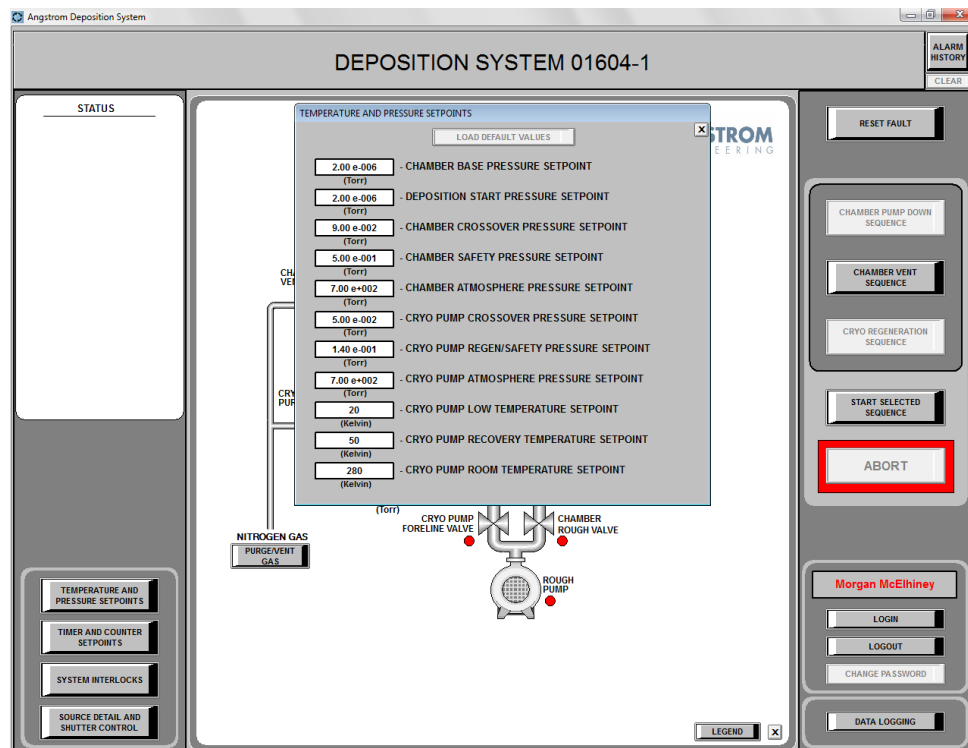


Figure 2.16: Diagram of the Temperature and Pressure Setpoints Menu.

Important setpoints to notice are the system base pressure and deposition start pressure, which should be the same value. This is the pressure at which the system is

considered “pumped down” and allows for depositions to be started. The crossover pressure setpoint is where the system switches from pumping using the roughing pump to the cryopump. The next useful menu is the “SYSTEM INTERLOCKS” menu. This menu, shown in Fig. 2.17, displays current interlock states.

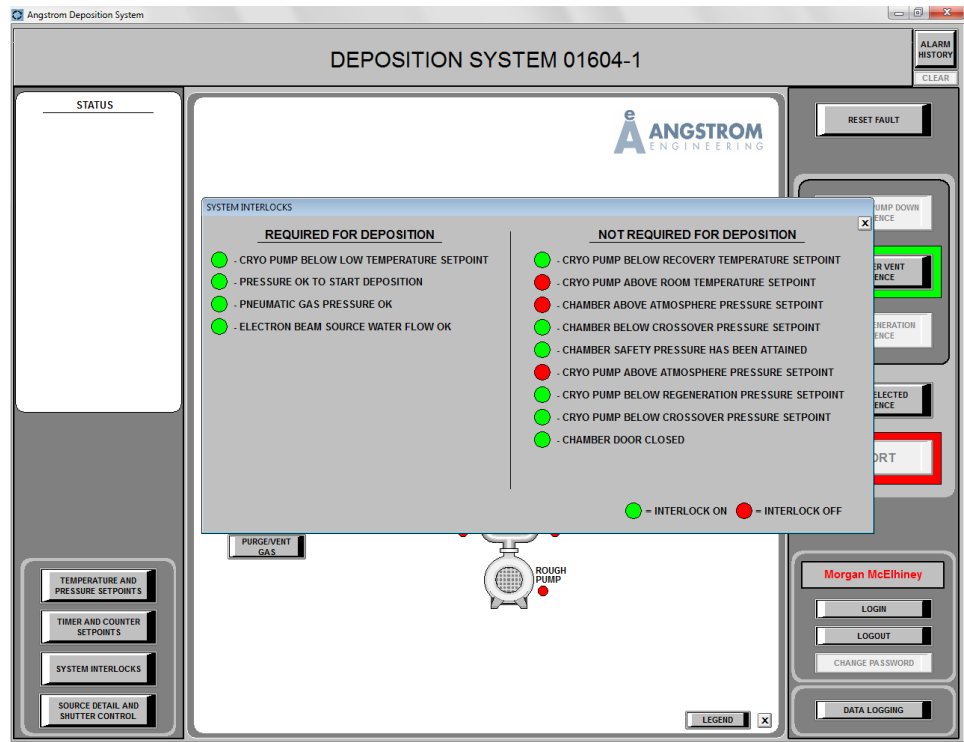


Figure 2.17: Diagram of the System Interlocks menu.

To start a deposition, the four interlocks on the left side of this menu must all be green.

The last menu on the left is arguably the most important. The “SOURCE DETAIL AND SHUTTER CONTROL” menu, shown in Fig. 2.18, contains all the information describing the source and source materials present in the chamber as well

as shutter and sample rotation information. It also contains the tooling factor formula, which will be discussed later.

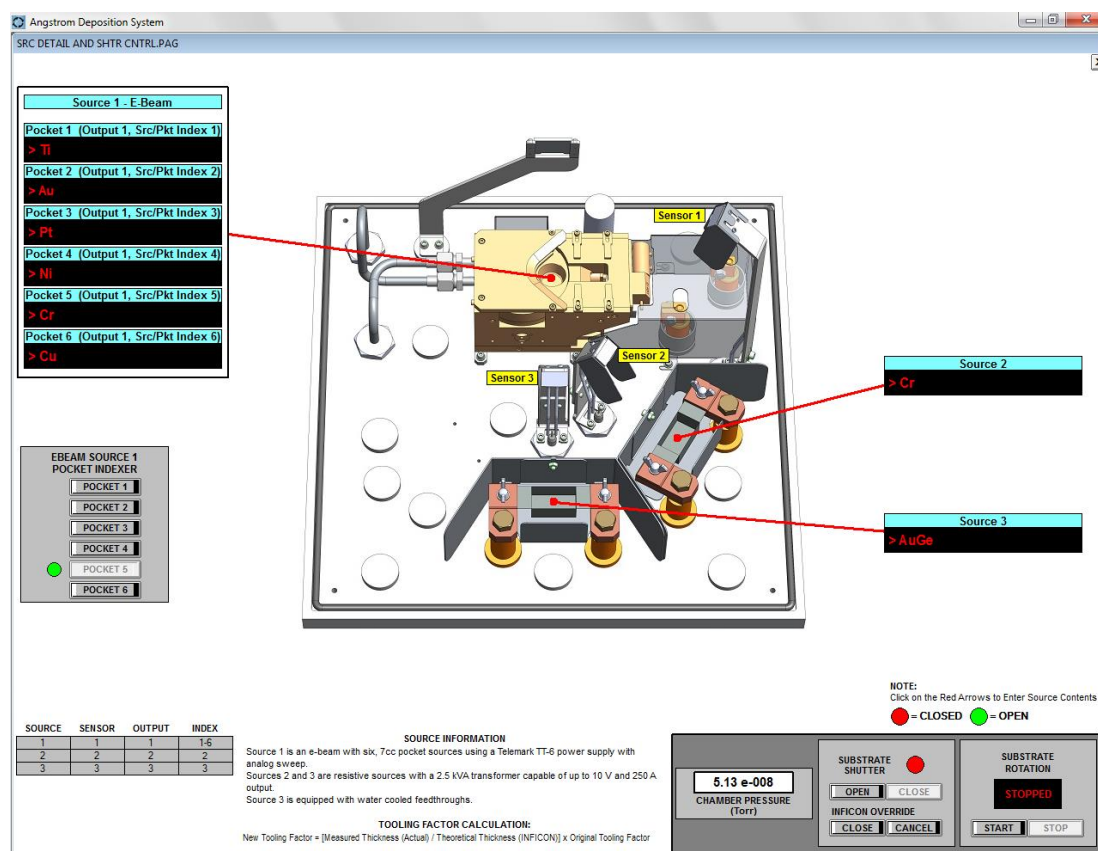


Figure 2.18: Drawing of the Source Detail and Shutter control menu.

The callout for “source 1 e-beam” shows the various materials in the six crucibles currently loaded into the system. The source 2 and 3 callouts show what materials are loaded into the two thermal sources. The e-beam source 1 pocket indexer button panel rotates the crucible carousel to a selected pocket. This can only be performed when the chamber is latched closed. The graphic in the center details the location of all the sources and sensors, in the chamber. The two panels on the bottom right control the

shutters and substrate rotation. The open and close buttons open and close the shutters. The Inficon override button forces the shutters to stay closed even if the deposition program attempts to open the shutters. It is important to confirm that this override is turned off otherwise the material will not deposit on the samples rendering the process useless. The start and stop buttons start or stop the substrate rotation manually.

Once it is confirmed that the system is in a normal state the system can be vented. To vent the chamber, click the “CHAMBER VENT SEQUENCE” button. This will cause the chamber vent menu, shown in Fig. 2.19, to pop-up.

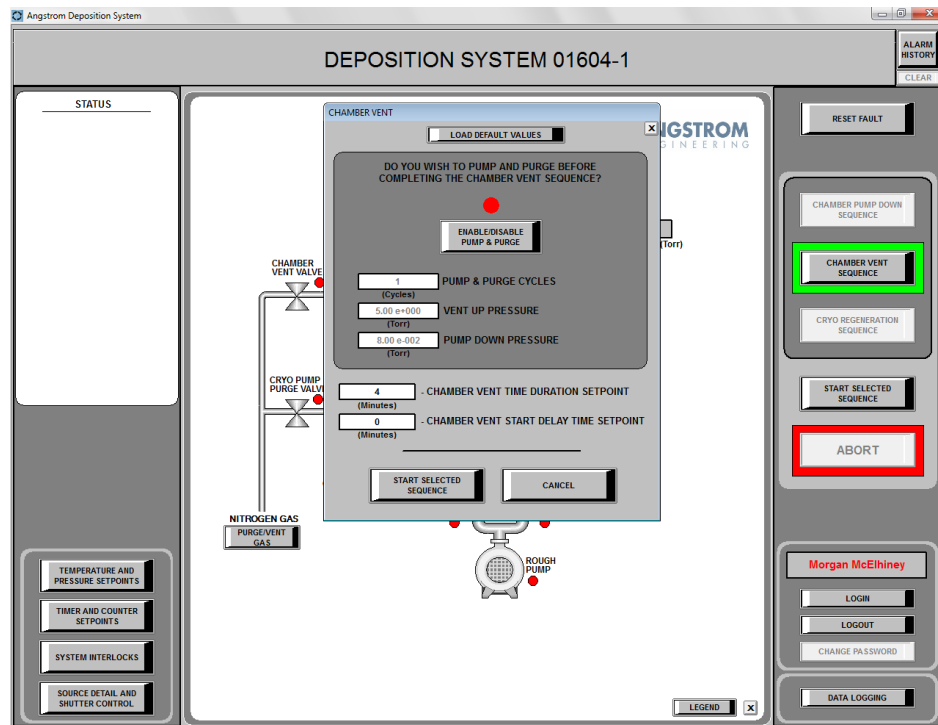


Figure 2.19: Diagram of the Chamber Vent pop-up menu.

This menu allows the user to a program cycle purge routine to reduce the number of toxic species from the chamber environment. As this system does not use toxic gasses or materials, a cycle purge is not necessary.

To start the venting process, click the “START SELECTED SEQUENCE,” button. This will close the cryopump gate valve and open the chamber vent valve to slowly introduce nitrogen into the chamber. At this point, open the two red latches, depicted in Fig. 2.20, on the chamber. This causes the chamber to pop open when the internal pressure reaches atmospheric pressure.

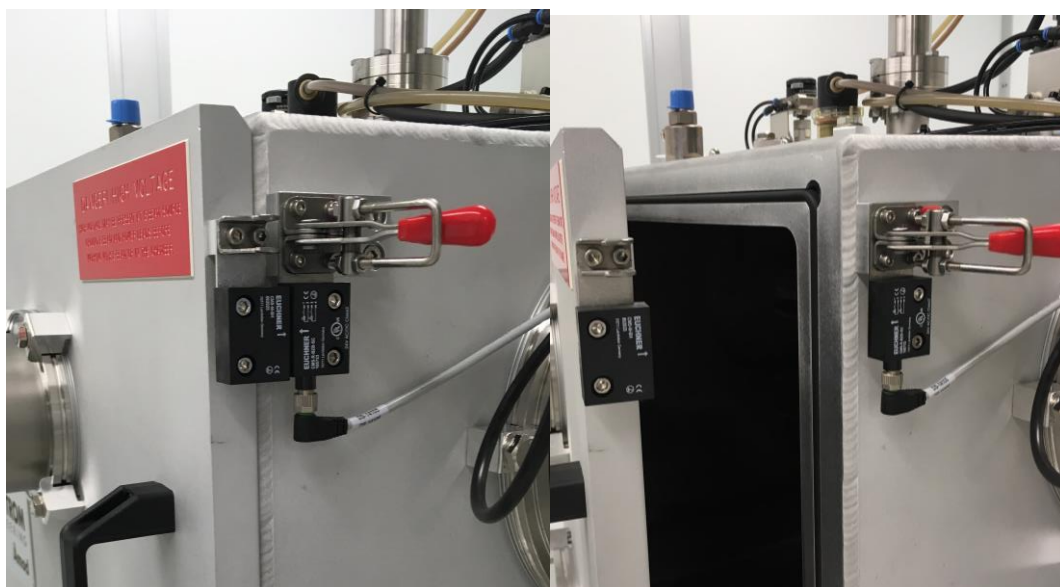


Figure 2.20: Unlatched chamber (left) before and (right) after reaching atmosphere.

When the chamber opens, the black magnetic sensor below the top latch informs the system that the chamber is open; therefore, ending the venting process.

With the chamber now open, samples can be loaded and sources can be changed or inspected. Figure 2.21 shows the three sources. The e-beam source and

crucibles are in the back of the chamber. Two thermal sources are near the front of the chamber. Each source has a crystal sensor. Each thermal source sensor is near each respective source. The e-beam source sensor is higher and closer to the sample plate to avoid interfering with the beam path.

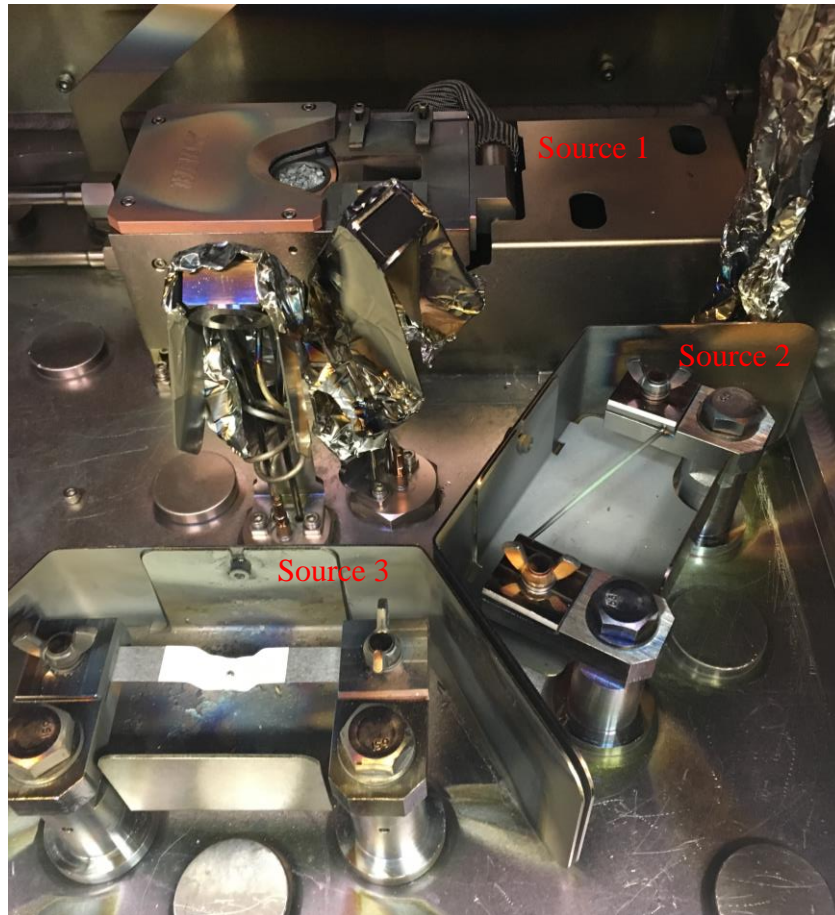


Figure 2.21: Illustration of e-beam chamber with crucibles and thermal sources.

Before performing a deposition, the sources should be checked for adequate fill level and cleanliness. Crucibles should not be changed or filled without permission of the equipment supervisor and should have a uniform melt at least half full. The

chromium crucible is an exception. Chromium does not melt and therefore sublimates rather than evaporation, therefore the pellets remain solid. The chromium crucible is shown in Fig. 2.21. Thermal sources can be changed and filled at the discretion of the user, but should be removed after use. Subsequent users are not responsible for other user's sources. If a source must stay in the chamber it should be covered with aluminum foil. When loading a thermal source, note the placement of the boat as well as the material, as this will affect deposition rate and tooling factor.

The sample plate, shown in Fig. 2.22, is located upside down on the top of the chamber, mounted to a water feedthrough spindle, which not only rotates but also cools the plate with water from the chiller.



Figure 2.22: Illustratioion of the sample holder mounted and unmounted on table.

To remove the sample plate from the chilled rotation mount, tighten the screws, shown in Fig. 2.23, on either side to expand the spring-loaded clamps.

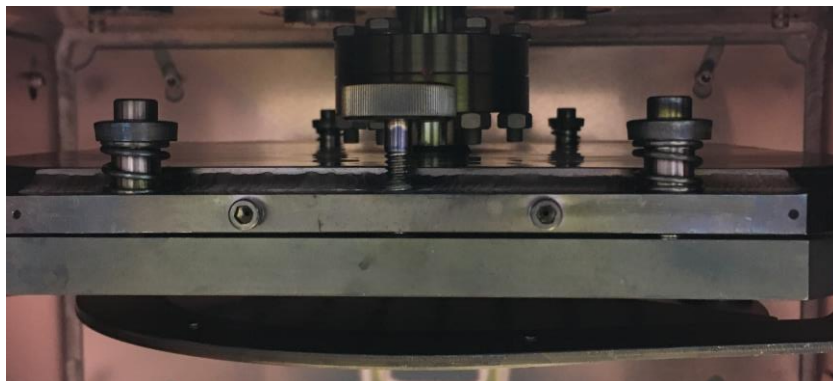


Figure 2.23: Side view of sample plate mount with springs and spacer screw.

Slide the plate straight out of the mount. Once removed, flip the plate over and place it on the wipe covered cushion on the workbench. Use the screws and clips to securely mount samples. For depositions with rotation, place samples as close as possible to the center of the plate. For stationary depositions, place samples so they will be above the appropriate source.

To clean any debris from the samples and holder, liberally spray the plate with the nitrogen air gun, then replace the plate in the holder. Once the holder is in place, loosen the screws until the springs are fully extended, then tighten them slightly so they don't vibrate.

Confirm that the sources are ready, samples are loaded, and check the chamber for any aggressive flaking or debris. Once ready, close the chamber doors and latch both latches. Click the "CHAMBER PUMP DOWN SEQUENCE," button, and the click, "START SELECTED SEQUENCE." This will start the pump down sequence. The cryopump should already be started and stable at this point. The roughing pump will start and pump down the roughing line. After 30s, the chamber rough valve will open and the chamber will begin to be pumped. Figure 2.24 shows

the state of the system as the chamber rough valve is opened. The rough pump is denoted as on by a green circle and the rough valve is denoted as open by a green circle. On the left of the window the pump down process is illustrated with the active step illuminated by green text.

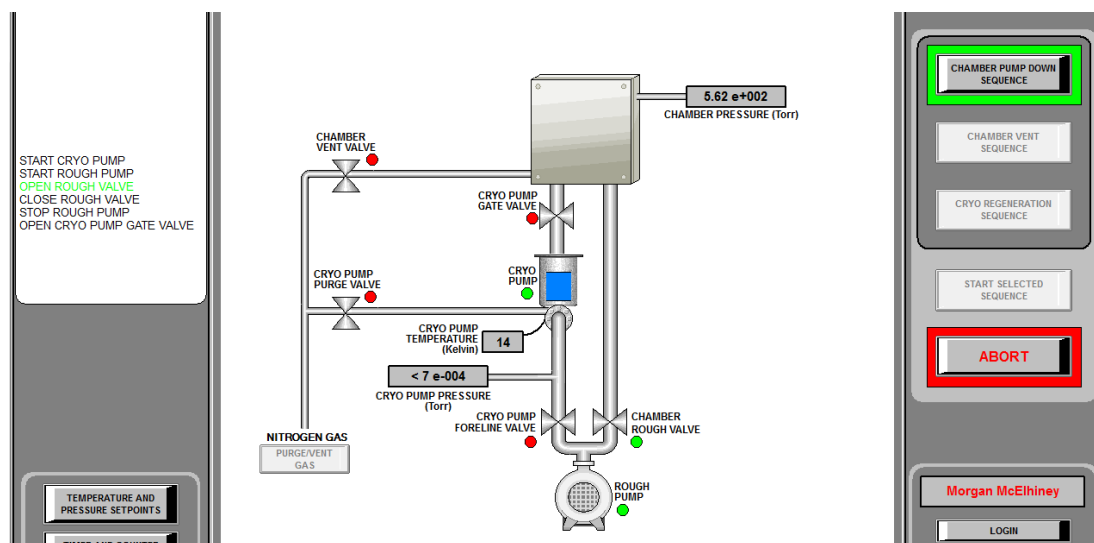


Figure 2.24: Drawing of system state during rough vacuum pumping.

Once the system hits the cryo crossover pressure setpoint, the chamber rough valve will close and the roughing pump will turn off. It is important for the roughing line to never reach an equilibrium state as it is a mechanical pump containing oil. If it reaches an equilibrium state, oil will backstream through the line. The crossover setpoint is set to reduce this phenomenon. Next, the cryopump gate valve will open exposing the cryo head to the chamber. The chamber pressure will rapidly drop and over time achieve base pressure and beyond. This system can achieve pressures into the low 10^{-8} torr region, or High Vacuum. Only 2×10^{-6} torr is required for deposition.

2.1.4 Inficon Deposition Software

The second software application needed for deposition is the Inficon deposition control application. This program controls the power supplies attached to the sources based upon feedback information from the crystal sensors. The software can only be accessed with a login. After logging in, you will be able to see the main page of the software, shown in Fig. 2.25.

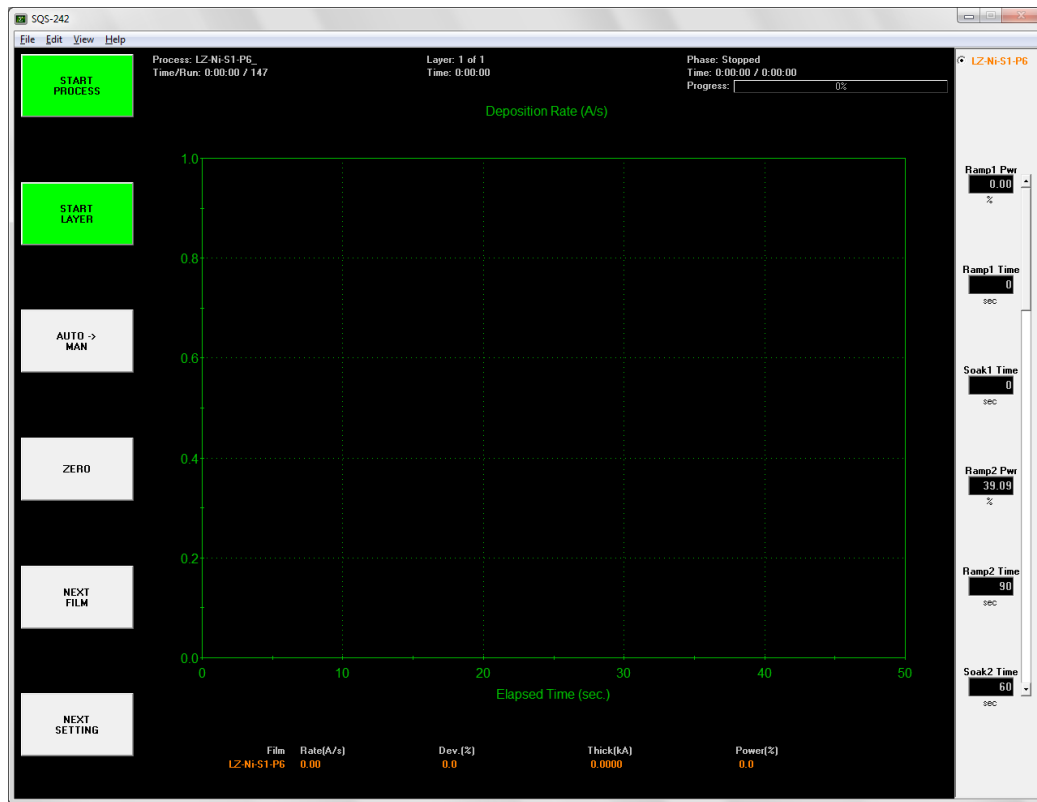


Figure 2.25: Capture of the Inficon Software Home Page.

The buttons on the left panel control various parts of the process. The “START PROCESS” button starts a process from the first layer. The “START LAYER” button starts a process from the currently selected layer. The “AUTO->MAN” button selects

whether the process will be controlled by the control loop or by manual power input during the deposition. The “ZERO” button sets the value of layer thickness to zero during the process effectively ignoring any material deposited previously. The “NEXT LAYER” button advances the process to the next programmed layer.

Across the top of the window shows various information concerning the deposition and process. The first section shows the selected process, the current total runtime, and the total runs of the process. A second section shows the current layer number and layer runtime. The third section shows the current process phase, current step time, and remaining time and percent. A bar along the right side of the window shows the current film at the top and all the menu parameters. Menu parameters will automatically scroll as the deposition progresses.

When preparing a deposition, the first step is to create a film, which defines how a specific material will be deposited. To open the film menu, click Edit -> Film. To create a new user specific film, select a similar film from the general films, prefixed with “Gen,” see Fig. 2.26.

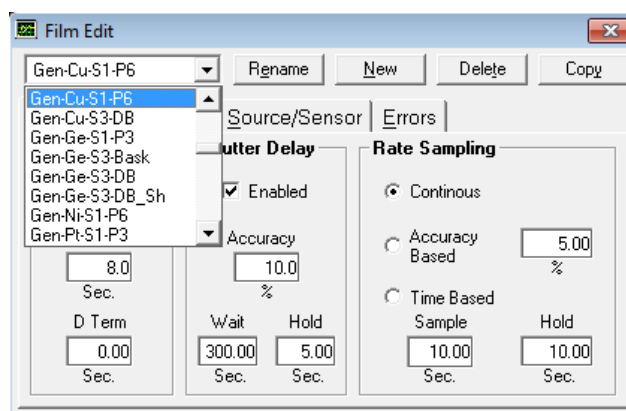


Figure 2.26: Capture of the General Film Selection in Film Menu.

After selecting the appropriate general film, press copy. This will bring up a labeling keyboard, see Fig. 2.27. Change the “Gen” prefix to your initials and press Enter.

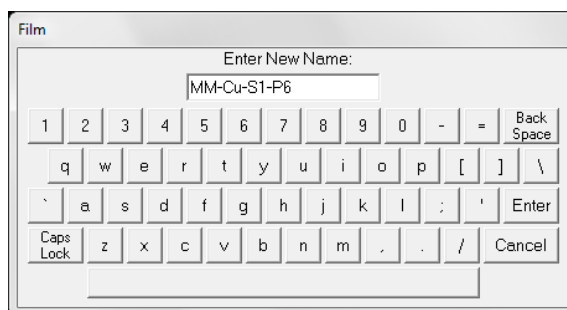


Figure 2.27: Capture of the Film Label Editor.

The components of the label include “initials-material-source-pocket.” Thermal source labels do not include a pocket label, as the sources do not have multiple pockets. After saving your user specific film it is important to inspect the parameters. Most parameters do not need to be changed from the general film. The first tab is the “Deposit” tab, shown in Fig. 2.28.

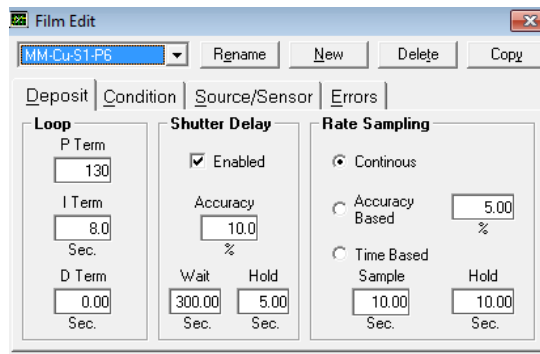


Figure 2.28: Capture of the Deposit Film Menu.

The section labeled “Loop” defines the PID parameters. The PID controller controls the feedback loop by changing the power of the source accordingly. *P* stands for proportional. This somewhat arbitrary variable controls how much the power will change due to a deviation. The *I* stands for integral. This parameter has units of seconds and relates to how many seconds in the past to average to filter out noise. The *D* term is derivative and is used to filter out oscillations. This term is almost always set to zero.

The second panel describes shutter delay. Shutter delay occurs between the pre-condition and deposition steps. Since the precondition does not use the controller, shutter delay allows for the control loop to stabilize before opening substrate shutters. When enabled, the deviation must be within the set percentage, within the allotted wait time, and stay within the allotted deviation for the set hold time. Once the rate is confirmed, the shutters will open starting the deposition. As the system does not contain crystal shutters, rate sampling should always be set to continuous.

The second tab is the “Condition” tab, shown in Fig. 2.29.

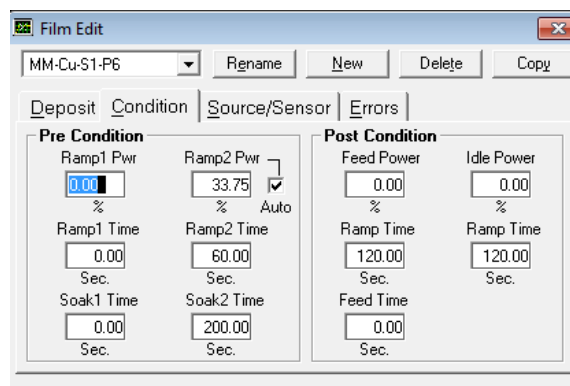


Figure 2.29: Screen Shot of the Deposit Condition Menu.

The pre-condition controls how the power is ramped from an off state to the deposition power. In evaporation “Ramp1” is rarely used but has some applications such as out-gas reduction and boat preservation. “Ramp2” brings the power from the “Ramp 1” power to the setpoint, “Ramp2 Pwr”. The “Auto” checkbox, when checked, will automatically take the power at the end deposition of this exact film and set it as the value for “Ramp2 Pwr”. The ramp time determines the length of the ramp. The soak time determines how long the power will be held at the ramp power setpoint before moving to the next step. The soak step is designed to allow the material to hit an equilibrium temperature and burn off any surface contaminants or trapped gasses.

The post-condition ramps the power down to a specified power and then holds the power typically at zero. This allows the melted material to slowly cool to a solid. It must be cooled slowly so the boat or crucible does not crack from thermal contraction. Also, if a crucible does not fully solidify before the indexer rotates, the material could spill and effectively weld the carousel in place.

The “Source/Sensor” tab is the third tab, see Fig. 2.30.

Source			
Material	Max. Power	Slew Rate	
Copper	50.00%	1.0%	

Sensor Tooling (%)			
1	2	3	4
99.5	100.0	100.0	0.0
5	6	7	8
0.0	0.0	0.0	0.0

Figure 2.30: Capture of the Source/Sensor Menu.

The “Material” drop down menu contains various deposition materials. Setting the appropriate material calibrates the sensor to be able to read deposition rate for the specific material’s density. The “Max Power” setpoint controls the highest value the power can reach during a deposition. This is important in a few cases: when a source runs out of a material, the controller will try to increase power forever but never rate will not increase. Setting a max power will alert the system that something is wrong when the power gets too high. It also protects the boats and crucibles from overheating. In thermal sources, it should be set so that the total output power through the specific boat resistance does not exceed the rated power of the source. The slew rate controls how fast the power can change per second.

Sensor tooling factor is a ratio between the deposition rate on the sensor and the deposition on the actual sample. This parameter is based on the sensor and sample distance and angle differences from the source charge. This should be adjusted by running test samples and mechanically or optically measuring the film thickness. The formula for calculating the tooling factor is:

$$New\ Tooling\ Factor = \frac{Measured\ Thickness}{Theoretical\ Thickness} \times Original\ Tooling\ Factor \quad (2.1)$$

The tooling factor should be set for the crystal specific to the chosen source.

The fourth and final tab is the “Errors” tab, shown in Fig. 2.31.

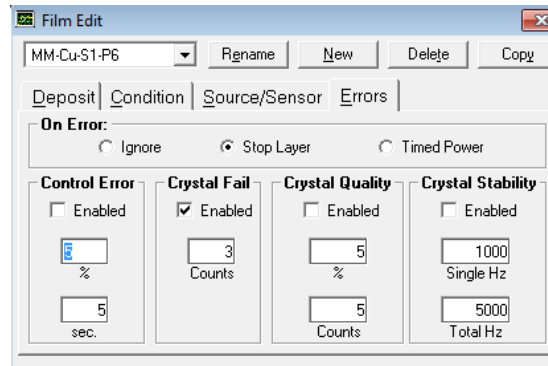


Figure 2.31: Screen capture of the Errors Menu.

This menu controls how the system will react to various errors. The “On Error” selector chooses what will happen when an error occurs. “Ignore” and “Stop Layer” are intuitive. “Timed Power” calculates the remaining time at the last known rate and attempts to complete the deposition. The only commonly used error condition in our systems is “Crystal Fail” error. When the crystal can no longer reliably determine deposition rate, the system will enter an error state. “Control Error” is based on deviation. “Crystal Quality” and “Crystal Stability” are based on the specific response of the crystal.

Once the film has been setup, close the film menu. Open the process menu by clicking Edit -> Process. In the process menu, create a new process the same way the new film was created. Open the general process, then press copy and edit the existing line to represent the process. Processes can deposit stacks of films and labels should clearly describe the succession of films. The process menu has six tabs, but four of those tabs are called from the film menu, as shown in Fig. 2.32.

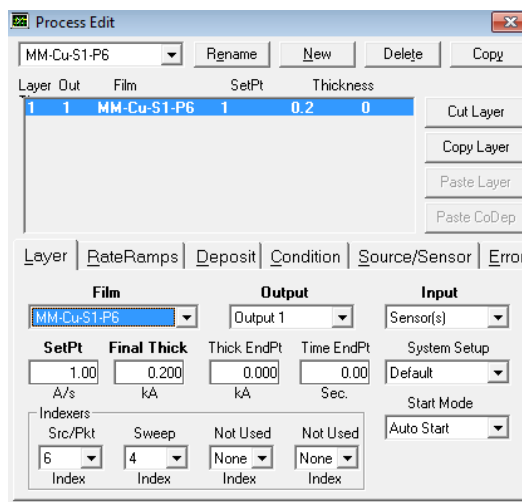


Figure 2.32: Screen shot of Process Menu with Layer Tab Selected.

To add multiple layers, copy and paste the existing film. To create a co-deposition, copy a film and then change the exiting source to a new source and press “Paste CoDep”. This will make the two layers deposit at the same time. If you try to paste a CoDep without changing the source it will throw an error because a CoDep relies on having two sources which can deposit materials at the same time.

In the “Layer” tab, the first dropdown menu labeled “Film” is used to select a film from the film menu. When selected, all the information form the specific film will be accessible from the process menu while highlighted in the above process film list. The output dropdown is used to select the source. The input dropdown selects either “Sensors” or “Timed Power”. Selecting Sensors controls the system with a feedback loop. Timed power holds a specific power for a set amount of time.

The “SetPt” box sets the desired rate for the deposition, which is material sensitive. Slower deposition rates often give smoother films. Most metals should not be deposited at rates higher than 1 Å/s. The “Final Thick” box determines the end of

the deposition. The “Thick End” point will stop a specific film during a CoDep. The “Time EndPt” is the desired time to deposit during a timed power deposition. When timed power is selected, the “SetPt” box will change from units of rate to units of % Power. There is only one system configuration, so the “System Setup” dropdown can only be set to default. In the “Indexers” section, the first box “Src/Pkt” is used to select the indexer position which holds the specific material to be deposited. Double check this value on the “Source/Shutter” detail page in the Ångstrom Software. The “Sweep” box selects a preconfigured sweep from the sweep controller. The sweep details are outlined on the system.

The final Tab to be discussed is the “Rate Ramp” tab, shown in Fig 2.33.

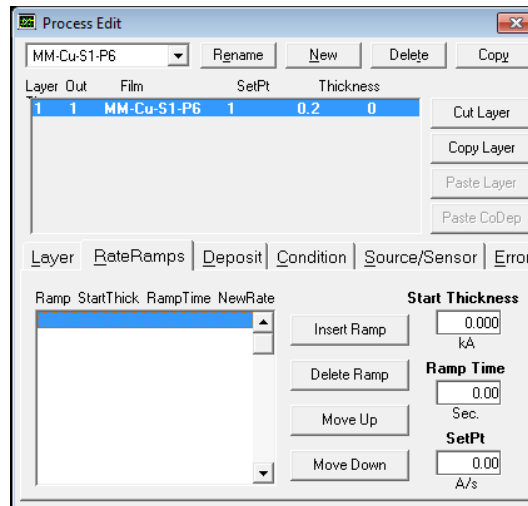


Figure 2.33: Screen capture of the Rate Ramps Tab.

On this tab, rate ramps can be added to the process flow, starting at a specific thickness. The deposition rate can be increased over a specific amount of time to reach a new desired rate. This may be useful to have a slow deposition rate at the beginning

of a deposition, which increases the rate after a base layer has been deposited to finish the deposition faster. Rate ramps can also be used to address internal film stress issues.

After developing all the necessary films and configuring the whole deposition, confirm the whole process by clicking through all the films and double checking the parameters and set points, close the window. When exiting the process window, a pop-up, see Fig. 2.34, will prompt you to change the process to the process selected before you closed the window.

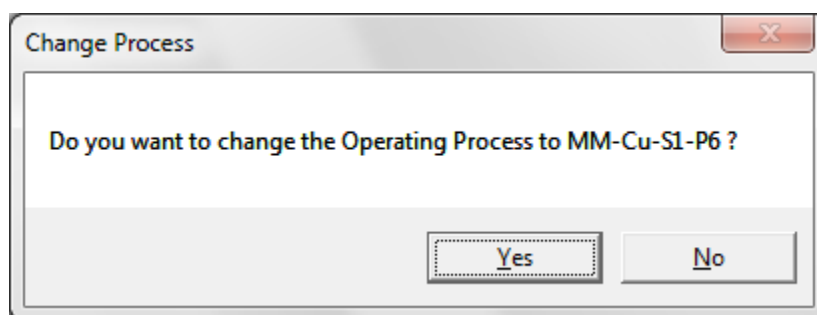
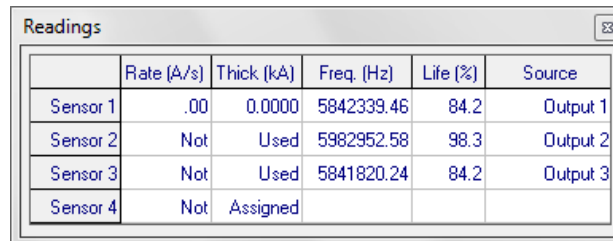


Figure 3.34: Screen capture of the Change Process Prompt.

Selecting “Yes” will change the current process to the mentioned process which is the last one viewed. Pressing “No” will leave the previous deposition selected.

Once you confirm the appropriate process is selected, press the start deposition button. The source will turn on and start ramping based upon pre-condition parameters. In evaporation, there will be a significant portion of the pre-condition where the crystal rate monitor will read close to zero. After the charge melts or reaches a sublimation point, the crystal will start to read a rate. If the rate does not reach an expected value before reaching shutter delay, there could be an issue with the system or source, or the power needs to be adjusted.

After the pre-condition, the feedback loop will take over. The system will attempt to achieve a well-controlled deposition rate with minimal deviation from the set point. Although evaporation often holds steady rates, there will always be some noise in the control system. Noise can be from the source, the charge, or the crystal. Crystal noise increases as the crystal life decreases. To check the crystal life, click View -> Sensor readings. This will show the Sensor Life for each sensor, shown in Fig. 2.35. The sensors correlate to the appropriate sources.



The screenshot shows a window titled 'Readings' with a table containing sensor data. The table has six columns: Sensor, Rate (A/s), Thick (kÅ), Freq. (Hz), Life (%), and Source. There are four rows of data for Sensor 1 through Sensor 4.

Sensor	Rate (A/s)	Thick (kÅ)	Freq. (Hz)	Life (%)	Source
Sensor 1	.00	0.0000	5842339.46	84.2	Output 1
Sensor 2	Not	Used	5982952.58	98.3	Output 2
Sensor 3	Not	Used	5841820.24	84.2	Output 3
Sensor 4	Not	Assigned			

Figure 2.35: Screen capture of the Sensor Life Readings.

Sensors that only encounter one material can be used until very low life percent, but since this evaporator is used often, with many materials, crystal sensors need to be replaced well before 50% remaining life. Sensors can be changed by an equipment supervisor.

Once the controller achieves rate within the deviation allotted by the shutter delay parameters, the substrate shutters should open. It is important to observe all the material pre-conditions, but the system can be left alone for long periods of deposition. However, the user is responsible for the system during any deposition. The system is not perfect and depositions do fail, which can ruin samples and damage the system.

After completing a deposition process, vent the chamber, ground the source, remove samples from the platen, cover any vacant screw holes, replace the sample platen, and pump the chamber back down. Once the pump down process begins, exit the Inficon software and log out of the Ångström System Software.

2.2 Åmod Sputtering System

Although similar, the Evaporation system and the sputtering system have major differences in key areas. This section will include the setup and operation of the sputtering system, but will only describe differences from the evaporator in detail.

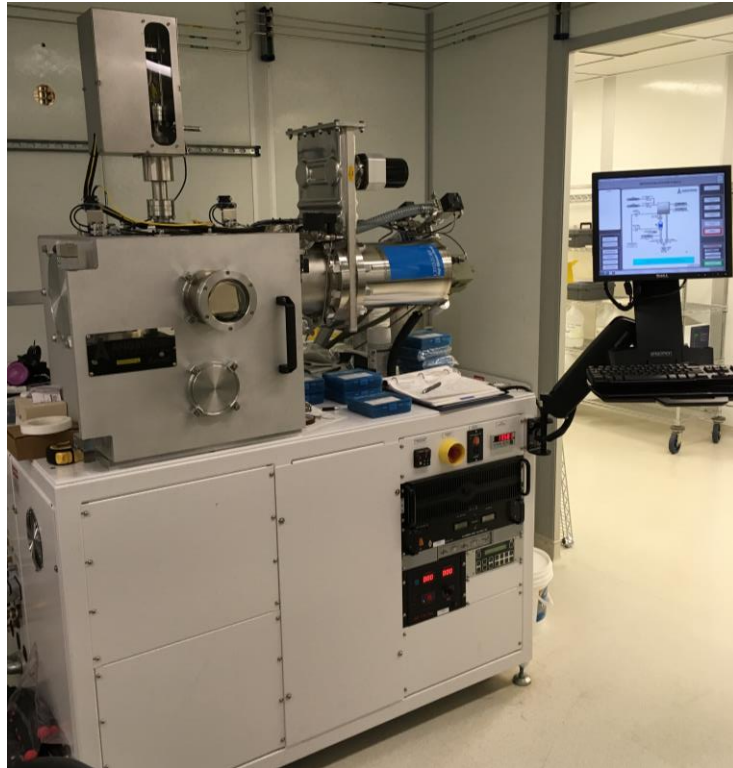


Figure 2.36: Illustration of the Åmod Sputtering System.

2.2.1 Safety and System Checks

The roughing pump and the compressor are identical to the roughing pump and compressor on the Evaporator. The specific units are to the left of the Evaporator units. The chiller on the sputterer is an older model Thermoflex 5000, shown in Fig. 2.37.



Figure 2.37: Illustration of the Thermoflex 5000 chiller on Sputter chiller loop.

This chiller cools water for the Sputterer and the Covap II. When checking the system, confirm that the setpoint is at 15° C. Sometimes this setpoint is changed due to environmental factors. Press the down arrow to check the system pressure; it should be around 65 psi. The system operates between 50-60 psi, but since there are two systems attached the pressure drop requires the source pressure to be higher than 60 psi. Press

the down arrow again to see the flow rate, which should be around 4.0 Lpm. On the outlet side of the system, check the pressure gauge, like the evaporator, and confirm the pressure is between 50-60 psi.

Sputtering requires process gasses to strike a plasma. There are three gas cylinders to check before operating the system. The argon and oxygen tanks are located along the wall in the end of the back chase. The two tanks on the right are the specific tanks for the sputterer, shown in Fig. 2.38 (a). The nitrogen tank is in the clean room behind the system, see Fig 2.38 (b). Confirm adequate tank pressures greater than 100 psi and line pressure 10-20 psi. The oxygen and nitrogen lines are attached to the same system input and cannot be operated simultaneously. They can be switched by a system supervisor.



Figure 2.38: Pictures of (left) Oxygen and Argon Tanks and (right) Nitrogen Tank.

2.2.2 Basic System Operation

Like the evaporator, the sputterer has a few rack units mounted to the front of the system. The emergency stop, substrate rotation controller, computer, and cryo temperature gauge are the same. The first panel, at the top left, is the substrate heater controller, see Fig 2.39. As opposed to the evaporator, the sputter substrate holder is heated not cooled to promote higher reaction rates during reactive sputtering. Note: substrate heating should only be used with permission from an equipment supervisor.



Figure 2.39: Illustration of the Substrate heater controller.

Below the computer is the DC source, shown in Fig. 2.40.



Figure 2.40: Front panel of the DC Sputtering Source.

This source supplies power to the left sputtering target and is labeled source 1. DC sputtering is only effective with metal targets because insulators will build up charge once biased. Confirm the power switch is in the on position before starting a deposition.

The next component on the rack is the RF matching unit, see Fig. 2.41.



Figure 2.41: Front panel of the RF Matching unit.

The matching unit adjusts the impedance of the RF load to limit back reflections which could be harmful to the source. Before system operation confirm that the power is in the on position and both mode switches are in the Auto position.

The RF source is in the bottom left corner of the rack, as shown in Fig. 2.42.



Figure 2.42: Front panel of the RF Sputtering Source.

This source supplies the right target in the system and is labeled “source 2”. Before operation, confirm that the power switch is in the “on” position.

The final unit is the VAT pressure controller, see Fig. 2.43.



Figure 2.43: Front panel of the VAT Adaptive Pressure Controller.

This controller relies on feedback from the process pressure gauge and controls the position of the cryo gate to maintain constant pressure during deposition. Before system operation, confirm that the remote mode is selected. Also, confirm the nitrogen pressures are correct on the two regulators for pneumatic and vent nitrogen on the wall.

2.2.3 Ångstrom Engineering System and Software

The home screen for the sputterer, shown in Fig. 2.44, looks similar to the Evaporator except for some key differences.

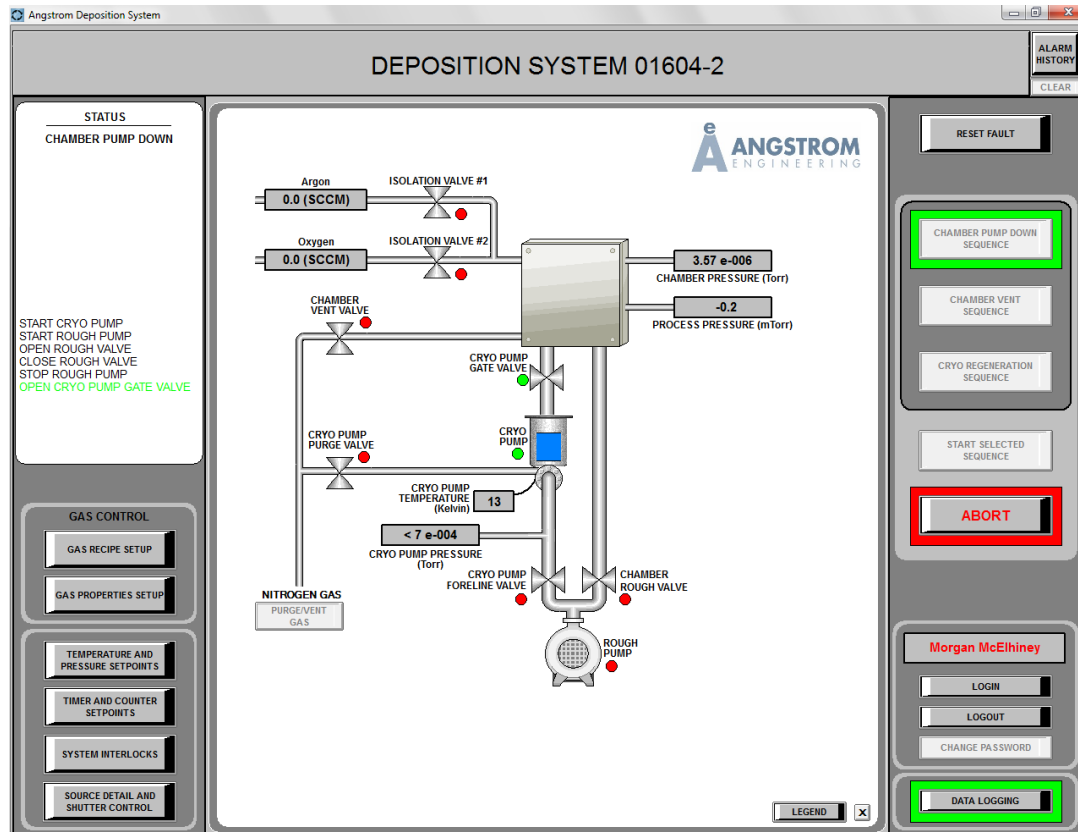


Figure 2.44: Drawing of the Sputter System Home Page.

The sputterer needs to flow process gasses therefore the system has gas inlets. Each inlet has an isolation valve to seal the line when the gas is not in use. Each gas needs to be flowed at a specific rate; therefore, a mass flow controller (MFC) is used on each gas line to control the specified rate. There is also a process pressure gauge which sends information to the adaptive pressure controller; the cryopump gate valve is variable on the sputterer.

The “GAS RECIPE SETUP” button is used to set specific flow and pressure values to be used by various processes, see Fig. 2.45.

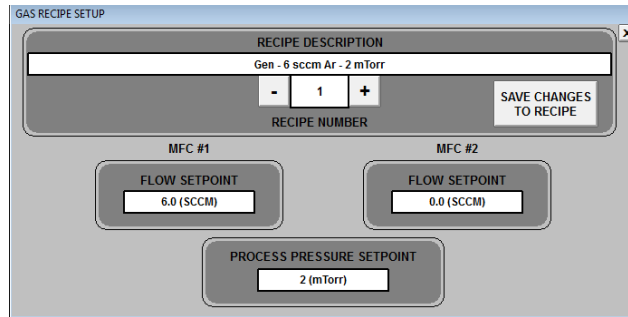


Figure 2.45: Screen capture of the Gas Recipe Setup Menu.

Each gas recipe has a flow rate for each gas as well as a process pressure set point. MFC #1 is always argon, which introduces a physical element to the plasma. MFC #2 is either oxygen or nitrogen, which supplies a reactive element to the plasma. Recipe #1 is used for most non-reactive sputtering processes and flows 6 sccm of argon as no reactive element is required.

When utilizing a reactive component, different gas ratios and pressures need to be developed. These parameters are deposition specific and need to be developed experimentally. The “GAS PROPERTIES SETUP” menu, see Fig 2.46, is used to calibrate the MFCs to specific gas properties, as gasses have different densities. The correction factor is a ratio comparing the gas to Nitrogen.

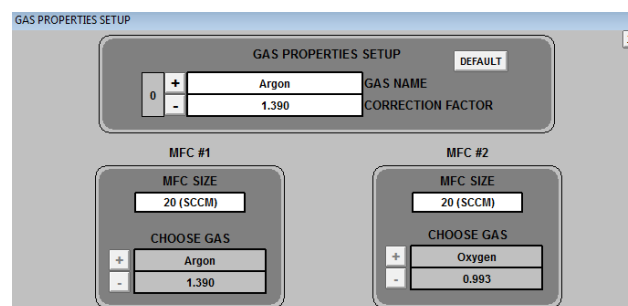


Figure 2.46: Screen capture of the Gas Properties Setup Menu.

MFC #2 is fed by two gas lines, oxygen and nitrogen, each line has a shutoff valve prior to a “T” and can be switched by an equipment supervisor. Please check the current gas listed in the system software before performing a reactive deposition.

The “SOURCE DETAIL AND SHUTTER CONTROL” menu, see Fig. 2.47, is similar to the evaporator but only shows the two sputtering targets rather than the evaporation sources.

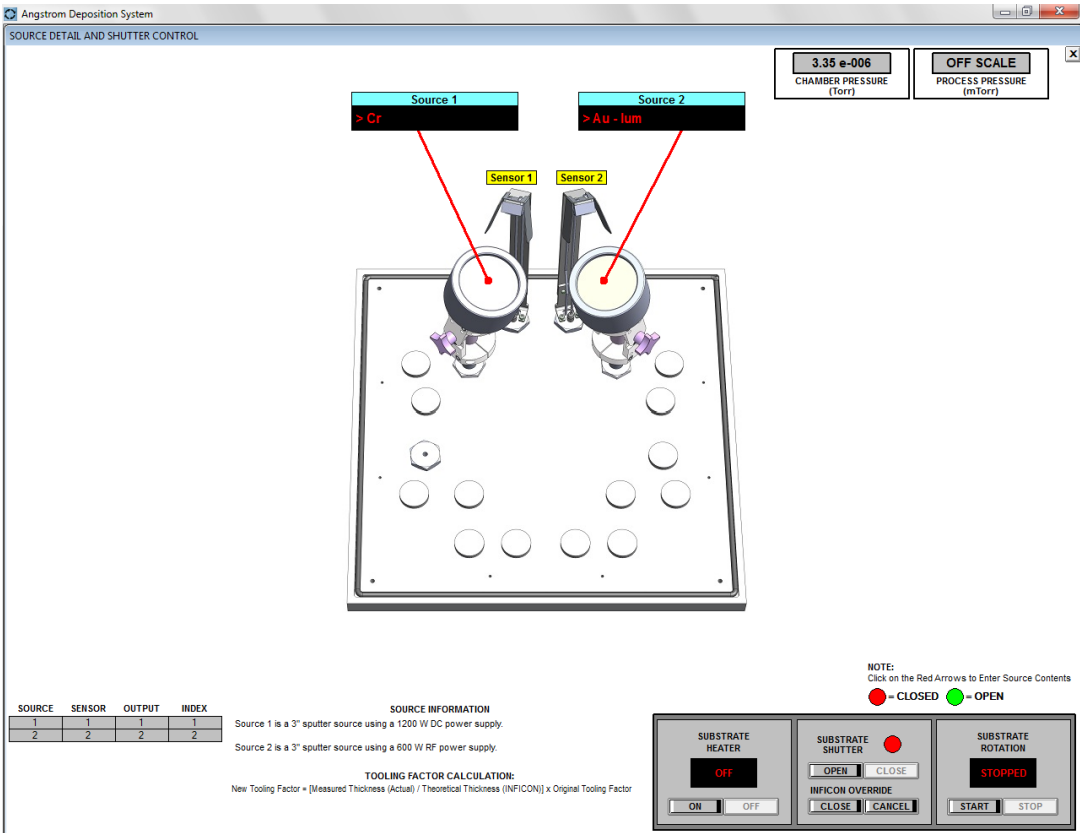


Figure 2.47: Drawing of the Sputter System Source Detail and Shutter Control Menu.

Once the chamber is vented, the inside of the system can be seen in Fig 2.48.



Figure 2.48: Image of the Sputtering Targets and Crystal Sensors.

The system has two targets. The left target is controlled by the DC source, and the right target is controlled by the RF source. Source targets can be easily changed. To change a target start by removing the outside collar by twisting the whole collar counterclockwise. This will reveal a secondary collar, as shown in Fig. 2.49. Remove this collar the same way.



Figure 2.49: Illustration of the Secondary Target Collar.

After the second collar is removed, gently pry the target off the assembly with a small flat head screwdriver, as shown in Fig. 2.50.

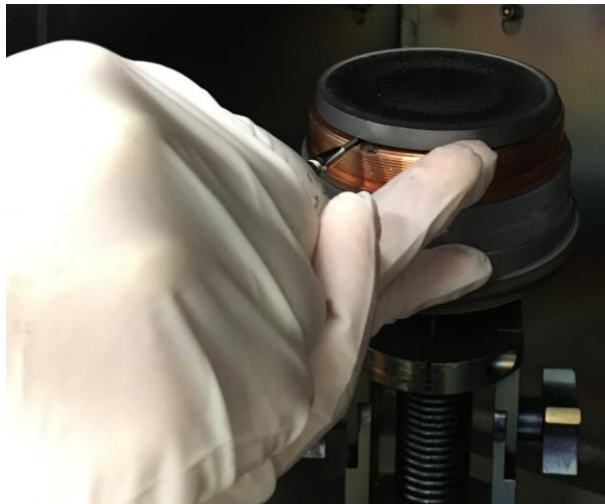


Figure 2.50: Demonstration of Target Removal.

Replace the existing target with the desired target. If thermal issues are suspected, apply a small amount of thermal paste to help thermally conduct the heat

from the target to the below water-cooled surface. Collapse the outer shield on the secondary collar and carefully replace. To avoid cross threading the delicate copper threads, set the collar on the threads and rotate counterclockwise until you feel the threads line up. Then, carefully tighten the collar clockwise. It does not require too much force. Once the inner collar is tight, pull down the shield to cover any exposed copper. Replace the outer collar. While tightening the outer collar, adjust the stop ring, see Fig 2.49, so the spacing between the two collars equals the thickness of the spacer, shown in Fig. 2.51.

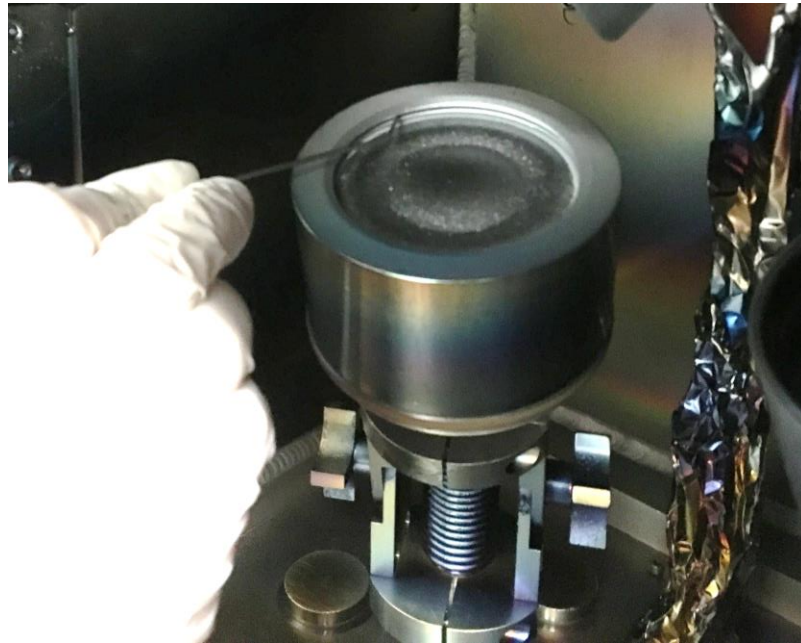


Figure 2.51: Demonstration of Checking Collar Gap with Spacer.

After setting up the correct source with a desired target, cover the other source with the provided shielding sleeve. Make sure the gap in the shield faces away from

the active target, see Fig 2.48. Place the glass dish on top of the target. This protects the other source and target from cross contamination.

The sample plate in the sputterer is different from the evaporator. To remove the plate, shown in Fig. 2.52 (a), open the shutters, use two hands to lift and rotate the plate. The plate should fall free, but might need to be shaken gently if stuck.

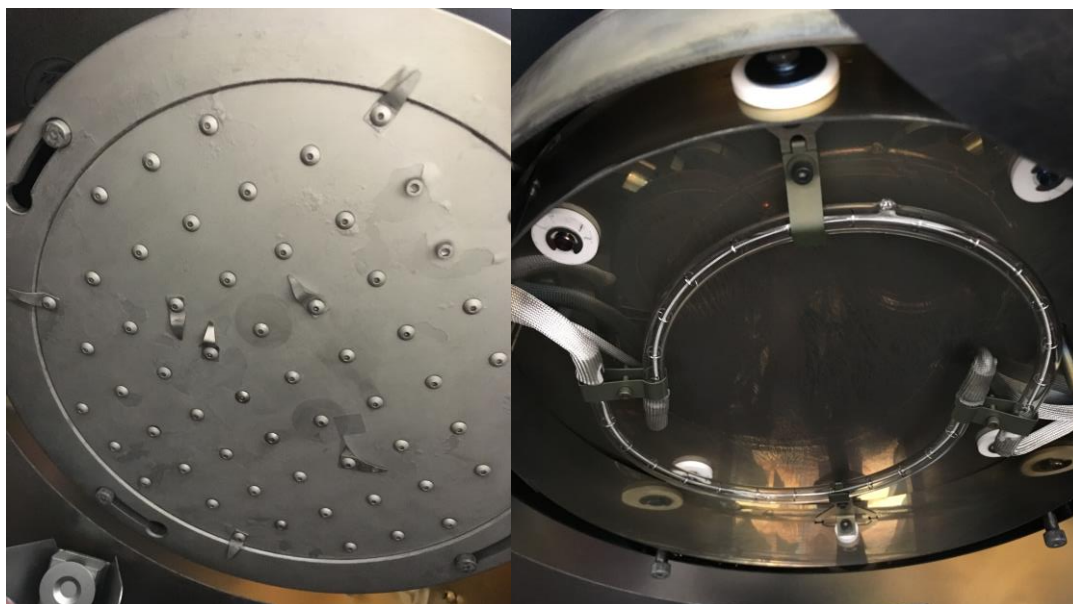


Figure 2.52: Illustrations of (left) Sample Plate and (right) Quartz Lamp Heaters.

With the sample plate removed, two quartz lamps can be observed, as shown in Fig. 2.52 (b). When working in the chamber with the plate removed be careful to not touch the lamps as they can break or fail due to contamination. To replace the sample plate, line up the pegs with the holes, insert the back peg into the far plate hole, and then the rest of the plate should easily swing into place. Rotate the plate to lock it.

After loading samples, confirming source configuration, and inspecting the chamber for debris and flaking, close the chamber and start the pump down sequence.

2.2.4 Inficon Deposition Software

The Inficon deposition software on the sputter system is almost identical to the software on the Evaporator. The first difference to consider when setting up a sputter process is during the pre-condition. Evaporation does not typically incorporate the first ramp. In sputtering the power needs to be increased rapidly to strike plasma; therefore, “Ramp1” is utilized to ramp the power to 5-15% power in ~5s. Then “Ramp2” brings the power to the desired rate power.

The “Layer” tab in the process menu, shown in Fig. 2.53, contains the only major differences in the software.

Layer	Out	Film	SetPt	Thickness
1	1	KRL-Cr-DC1	0.5	2 0

Buttons: Cut Layer, Copy Layer, Paste Layer, Paste CoDep

Tabs: Layer | RateRamps | Deposit | Condition | Source/Sensor | Error

Film: KRL-Cr-DC1

Output: Output 1

Input: Sensor(s)

SetPt: 0.50 A/s

Final Thick: 2.000 kA

Thick EndPt: 0.000 kA

Time EndPt: 0.00 Sec

System Setup: Default

Start Mode: Auto Start

Indexers: Source (1), Not Used (None), Gas Recipe (1), Not Used (None)

Figure 2.53: Screen capture of the Sputterer Layer Tab.

Everything on the tab is the same, except the outputs correlate to Source1 (DC) and Source2 (RF). In the Indexers section the source must be set again and must match the output. The gas recipe from the Ångström software is selected here as well.

Chapter 3

PVD APPLICATIONS

Although microfabrication techniques were developed to realized silicon transistor circuits, the industry has branched off into numerous directions. One of the largest offshoots is the optics industry. Optical communications has revolutionized the data transmission world. Optical Systems utilize transparent dielectrics and various diffractive surfaces can be fabricated utilizing PVD processes and other nanofabrication techniques, specifically 1D and 2D gratings.

3.1 Longwave Material Deposition

In optical systems, transparent materials with varying indices of refraction are highly useful for manipulating light. This section will explore the properties and deposition methods associated with Germanium (Ge) and Zinc Selenide (ZnSe).

3.1.1 Germanium and Zinc Selenide

Germanium is a common group IV element that behaves similarly to silicon and is often used in silicon photonics for lasers and detectors. Ge is fairly lossless and displays a refractive index (n) slightly higher than 4.0, see Fig 3.1. [9]

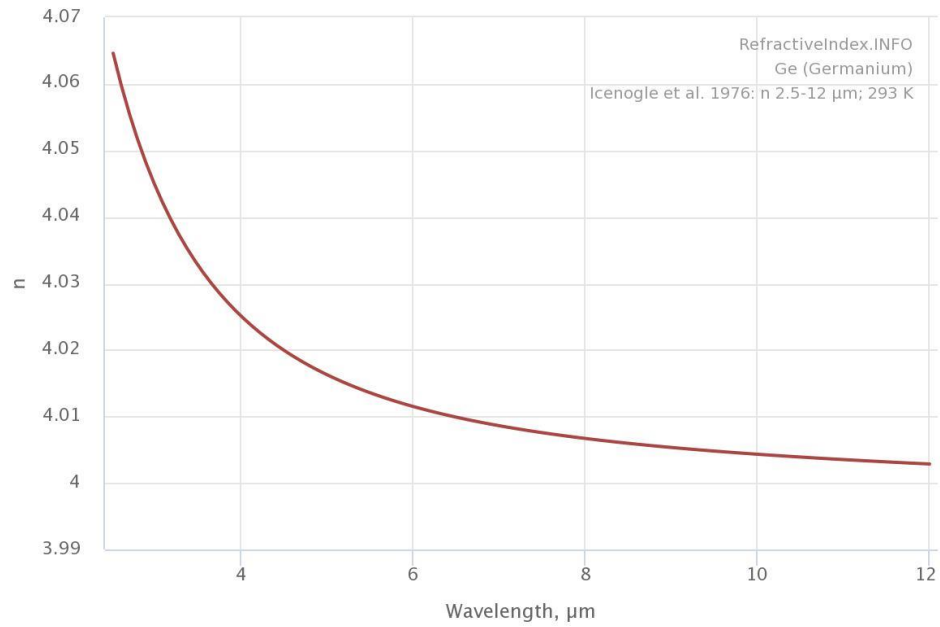


Figure 3.1: Plot of the Refractive Index of Ge.

ZnSe is a reddish material with a unique crystalline structure, Zincblende (cubic). It is a useful optical material and exhibits low loss. It has an average refractive index of 2.4, see Fig. 3.2. [10]

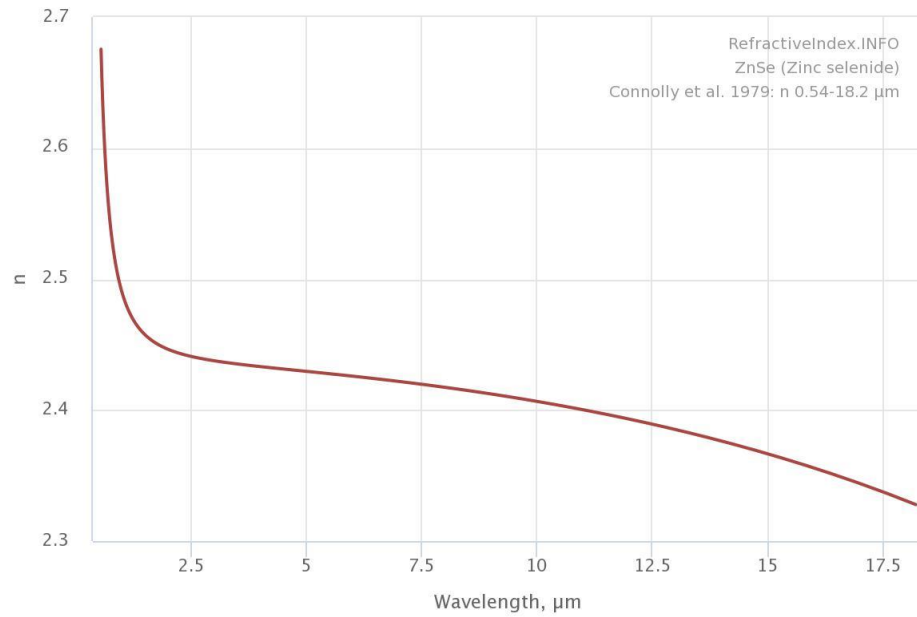


Figure 3.2: Plot of the Refractive Index of ZnSe.

3.1.2 Longwave Material Deposition

For all the films deposited in this chapter, either the Åmod sputterer or the Covap II was used. The sputterer operation was discussed in Chapter 2. This section will cover the operation of the Covap II, Fig. 3.3, from a research perspective rather than an operation perspective, The Covap source is identical to the thermal evaporation sources in the e-beam evaporation system. The system has one voltage source with two pockets, which can both be utilized, but not simultaneously.



Figure 3.3: Illustration of the Covap II Thermal Evaporator.

The system has a small reaction chamber with sources on the bottom and a sample plate with shutters on the top. The chamber is pumped by a roughing pump and TMP combination. The roughing pump starts and roughs the chamber through the TMP while the TMP is accelerating. The TMP can pump the chamber into High Vacuum regions, is water cooled, and controlled by the vacuum control module. Processes are controlled by an application specific Inficon deposition controller. It operates similarly to the Inficon software on the Åmod systems, and is linked to a single crystal rate sensor which is located between the two pockets.

For the deposition of Ge, alumina coated crucible hangers were used. A small crucible was formed by the manufacturer, Kurt J. Lesker. The crucible is formed around a length of resistive wire that spans the contact posts in the pocket. Current travels through the wire heating the crucible to extremely high temperatures $>1200^{\circ}\text{C}$.

Germanium pellets were purchased from Kurt J. Lesker. The pellets were placed in the crucible assembly attached to the source posts. The chamber was pumped down to a base pressure at low 10^{-6} torr pressures. New Ge pellets typically have a considerable layer of Germanium oxide coating the outside. Since the reaction chamber is small the outgassing from the new material must be considered when forming an initial melted charge. To slowly outgas the pellets, a slow Ramp1 is used ~ 6 min. This ramp starts at 0% power and ramps to the initial deposition power, rate $\sim 0.05\text{ Å/s}$. This allows the TMP to remove any excess gas from the chamber without tripping the deposition base pressure interlock.

After slowly depositing the material for a few minutes during the Ramp1 soak, to allow the chamber pressure to drop, Ramp2 brings the rate to 4 Å/s . The power set point for Ramp2 should be taken from previous runs. Crucibles are useful because

they have a somewhat uniform charge surface area and therefore reduce power deviation based on fill level.

ZnSe does not evaporate, it sublimates, and is a toxic material. It is also the most deposited material in the Covap system. A respirator must be worn when opening the reaction chamber. To sublime ZnSe, ZnSe pellets from Kurt J. Lesker are placed in a tantalum box source in the shorter pocket of the thermal source. The box is covered with a sieve cover which has holes to allow for the sublimated material to be released. New ZnSe pellets outgas, but not nearly as much as Germanium. Ramp1 is utilized to bring the boat rapidly to a low deposition rate. The power is then slowly increased by Ramp2 to a rate between 4-15 Å/s. This power is also recorded from previous experiments.

The ability to load both Ge and ZnSe at the same time is useful for depositing multilayer antireflective (AR) coatings. These coatings help couple light into a material with an index greater than free space. AR coatings are frequency dependent but are made broadband by increasing the number of layers.

Ge and ZnSe depositions are performed at high temperature. In the Covap chamber the sample holder is not cooled; therefore, the deposited film experiences a temperature gradient. This causes a film stress gradient, shown in Fig 3.4.

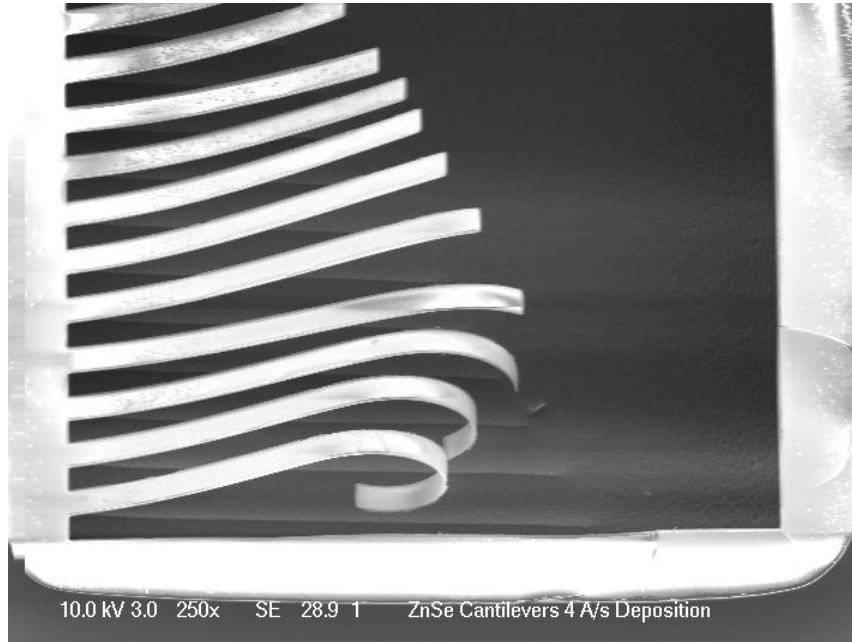


Figure 3.4: SEM of Warped ZnSe Cantilevers from Film Stress Gradients.

This film stress and the films natural poor adhesion qualities bring about the need for an adhesion layer. Chromium (Cr) was selected as an adhesion layer because of its ease of deposition. Thin layers of metals ~5nm barely effect the operation of optical elements. In the Covap, Cr adhesion layers are deposited by heating Cr plated rods with the thermal source. The Cr sublimates off the rod and is deposited like the other materials in the system. This step should be performed immediately before depositing another film without exposing the sample to atmosphere. Cr adhesion layers solved most adhesion issue with both ZnSe and Ge films.

3.1.3 Grating Fabrication

Periodic gratings are the simplest of diffractive optical elements The following process was utilized to fabricate optical gratings. A mechanically polished 1 mm thick

ZnSe window with a 25 mm diameter was prepared in a 500 W RF oxygen plasma to remove debris and trace organics. A layer of chromium (<5 nm) was deposited to promote adhesion. The Ge waveguide layer was then deposited at a rate of 4 Å/s through RF argon sputtering. The samples were washed in acetone, methanol, and propanol to remove any dust or debris. Negative liftoff photoresist (Futurrex NR9-1500PY) was deposited on the windows through a pipette and then ramped to 3,000 rpm at a rate of 1,000 rpm/s and spun for 45 s. The sample was then baked on a hot plate for 60 s at 150° C to remove any remaining solvents from the film. The photoresist was exposed using a periodic grating mask (2,800nm period with 35% fill factor) through contact photolithography. The resist exposure dose was 60 mJ/cm². The resist was baked again for 60 s at 100° C. The pattern in the resist was then developed in an RD6 (Tetramethylammonium hydroxide) solution for 15 s and then rinsed in deionized water. Excess photoresist was removed in a 150 W RF oxygen plasma. Another layer of Ge was deposited using thermal evaporation. The photoresist was lifted-off in acetone resulting in a patterned Ge grating (the resulting structure is shown in Fig. 3.5).

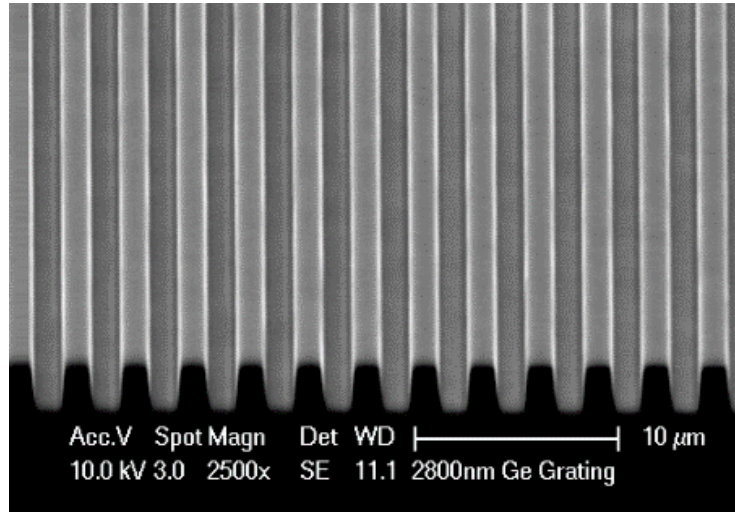


Figure 3.5: SEM of a 1D Germanium Grating.

Utilizing the same process but with a 2D grating mask a more complex grating structure was fabricated, shown in Fig. 3.6. It should be noted that the holes in the 2D gratings are round and not square. This is due to diffraction during the lithography process.

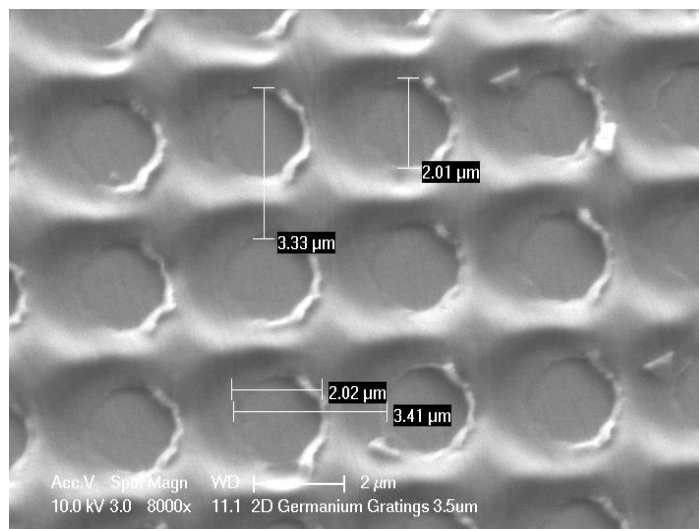


Figure 3.6: SEM of a 2D Germanium Grating.

REFERENCES

- [1] S. A. Campbell, *Fabrication Engineering at the micro- and nanoscale Fourth Edition*, Oxford University Press, New York, 2013.
- [2] *Vacuum Technology: It's Foundation, Formulae, and Tables*, Leybold AG, Export, PA 1992.
- [3] T. A. Delchar, *Vacuum Physics and Techniques*, Champman and Hall, London, 1993.
- [4] M. H. Hablanian, *High Vacuum Techniques: A Practical Guide*, M. Dekker, New York, 1990.
- [5] B. Champman, *Glow Discharge Processes: Sputtering and Plasma Etching*, Wiley, New York, 1980.
- [6] T. Iida, Y. Kita, H. Okano, I. Katayama, and T. Tanaka, "Equation for Vapor Pressure of Liquid Metals and Calculations of Their Enthalpies of Evaporation," *J.High Temp. Mater. Process* **10**:199 (1992).
- [7] Z.Y. Nuru et.al., "Optimization of AlxOy/Pt/AlxOy multilayer spectrally selective coatings for solar thermal applications," *Vacuum* **86** (2012).
- [8] O. Almen, G. Bruce, "Collection and Sputtering Experiments with Noble Gas Ions," *Nucl. Instrum. Methods* **11**:257, 279 (1961).
- [9] H. W. Icenogle, Ben C. Platt, and William L. Wolfe, "Refractive indexes and temperature coefficients of germanium and silicon," *Appl. Opt.* **15**, 2348-2351 (1976)
- [10] J. Connolly, B. diBenedetto, R. Donadio, "Specifications of Ratran Material," *Proc. SPIE* **0181**, Contemporary Optical Systems and Components Specifications, (1979)